Pergamon

Geochimica et Cosmochimica Acta, Vol. 67, No. 17, pp. 3101–3117, 2003

0016-7037/03 $30.00 + .00

PII S0016-7037(02)00929-8

An ultraviolet laser microprobe for the in situ analysis of multisulfur isotopes and its use in measuring Archean sulfur isotope mass-independent anomalies

GUIXING HU, DOUGLAS RUMBLE and PEI-LING WANG*
Geophysical Laboratory, 5251 Broad Branch Road, N.W., Washington, DC 20015

(*Received July* 16, 2001; *accepted in revised form April* 24, 2002)

Abstract—A laser fluorination microprobe system has been constructed for high-accuracy, high-precision multisulfur isotope analysis with improved spatial resolution. The system uses two lasers: (a) a KrF excimer laser for in situ spot analysis by ultraviolet (UV) photoablation with $\lambda = 248$ nm and (b) a CO_2 laser for whole-grain analysis of powdered samples by infrared heating at $\lambda = 10.6$ μm. A CO_2 laser is necessary for the analysis of interlaboratory isotope reference materials because they are supplied as powders. The $\delta^{34}S$ and $\delta^{33}S$ compositions of reference materials measured with a CO_2 laser fluorination system agree (± 0.2‰, 1σ) with the recommended values by the Sulfur Isotope Working Group of the International Atomic Energy Agency (Ding et al., 2001; Taylor, in press). The precision of replicate analyses of powdered sulfide minerals with the CO_2 laser is typically ± 0.2‰ (1σ) for $\delta^{34}S$.

The in situ fluorination of sulfides with a KrF excimer laser ($\lambda = 248$ nm) was validated by comparison of measurements of side-by-side laser craters and powders excavated from drill holes. Powders from drill holes were analyzed with the CO_2 laser. In situ laser craters and drill hole powders give the same $\delta^{34}S_{V\text{-}CDT}$ and $\delta^{33}S_{V\text{-}CDT}$ values within 0.2‰. The $\delta^{34}S_{V\text{-}CDT}$ and $\delta^{33}S_{V\text{-}CDT}$ values of both powders and in situ analyses are independent of F_2 gas pressure over a range of 15 to 65 torr. No dependence of $\delta^{34}S_{V\text{-}CDT}$ and $\delta^{33}S_{V\text{-}CDT}$ values on UV laser energy fluence has been observed. Mineral-specific fractionation of sulfur isotopes in analyzing pyrite, sphalerite, galena, troilite, and chalcopyrite has not been observed with a KrF excimer laser ($\lambda = 248$ nm). Test analyses with an ArF excimer laser ($\lambda = 193$ nm), however, gave fractionated sulfur isotope ratios.

A range of $\Delta^{33}S$ anomalies of from -1.5 to $+3.0$‰ in Archean samples from the North Pole district, Pilbara Craton, Australia, and from black shale of the Lokamonna Formation, South Africa, were verified by in situ analysis of individual pyrite grains with a KrF excimer laser. These results show that a combination of high-accuracy, high-precision analyses with improved spatial resolution permits locating and analyzing host minerals of non-mass-dependent sulfur isotope anomalies. *Copyright © 2003 Elsevier Ltd*

1. INTRODUCTION

Sulfur isotopes have been widely used as tracers in the study of igneous, sedimentary, hydrothermal, and biologic processes on the Earth (Ohmoto and Goldhaber, 1997). The development of in situ analytical techniques (Chaussidon et al., 1989; Eldridge et al., 1989; Crowe et al., 1990; Kelley and Fallick, 1990; Rumble et al., 1993; Beaudoin and Taylor, 1994; Greenwood et al., 2000) permits moderate to high spatial resolution for sulfur isotope analysis. Spatial resolution in turn provides detailed information for reconstructing the formation processes of minerals and rocks. Indeed, spatially resolved sulfur isotope analyses reveal features of mineral growth, recrystallisation, and metasomatism that are otherwise invisible. Beaudoin and Taylor (1994) observed sulfur isotope isopleths to crosscut growth zones in a metamorphic pyrite porphyroblast with their micro in situ laser extraction system (MILES) laser microprobe. A 74‰ fractionation in $\delta^{34}S$ across a 3-mm-thick pyrite-calcite vein from the Creede Formation, Colorado, was measured by Ilchik and Rumble (2000) with a CO_2 laser fluorination microprobe (Rumble et al., 1993). McKibben and Riciputi (1998) showed a variation of 89‰ in $\delta^{34}S$ across another section of the same Creede pyrite-calcite vein (sample number 2R224-A1.2) using an ion microprobe. Notable heterogeneity in $\delta^{34}S$ in 1-cm cross-sections of black smoker chimney walls was found using a laser SO_2 technique (Shanks et al., 1998). These effects are impossible to observe with conventional analytical techniques because bulk extraction by wet chemistry (Hulston and Thode, 1965) homogenizes sulfur isotope heterogeneity within the treated volume.

Fractionation of $^{34}S/^{32}S$ sulfur isotopes has been considered diagnostic of microbial activity in Archean sediments and metasediments (Monster et al., 1979; Thode and Goodwin, 1983; Hayes et al., 1992; Ohmoto et al., 1993; Shen et al., 2001) and in modern sediments (Canfield, 2001). But fractionation of $^{34}S/^{32}S$ by as much as hundreds of per mil in $\delta^{34}S$ is also produced by photodissociation of SO_2 (Farquhar et al., 2001a). Farquhar et al. (2000) proposed that photochemically induced sulfur isotope fractionations were transferred from the atmosphere to the hydrosphere and then to sediments in Archean time. Taking these observations and experiments into account, including the finding of mass-independent S isotope fractionations in sulfate aerosols in the present atmosphere (Romero and Thiemens, 2000; Thiemens, 2001), it is evident that at least three working hypotheses must be considered in the interpretation of sulfur isotope fractionations in sediments: (a) that $\delta^{34}S$ fractionations are caused by microbial action or other nonphotochemical processes, (b) that $\delta^{34}S$ fractionations are caused by photochemistry, and (c) that $\delta^{34}S$ fractionations are

* Author to whom correspondence should be addressed, (rumble@gl.ciw.edu).

caused by a combination of microbial and photochemical processes. Fortunately, the effects of ultraviolet (UV) photolysis can be distinguished from biologic fractionation because photodissociation produces non-mass-dependent fractionation among ^{32}S, ^{33}S, ^{34}S, and ^{36}S, while fractionation by biologic processes and other nonphotochemical processes is mass dependent (Hulston and Thode, 1965; Farquhar et al., 2001b; for a review of mass-dependent $^{34}S/^{32}S$ fractionation processes, see Ohmoto and Goldhaber, 1997; for ^{16}O-^{17}O-^{18}O fractionations, cf. Thiemens, 1999). In this context, an unambiguous interpretation of the significance of a $\delta^{34}S$ value alone can no longer be achieved without support from measurements of $\delta^{33}S$ and/or $\delta^{36}S$.

Non-mass-dependent fractionated sulfur isotopes have been measured in Archean and Paleoproterozoic terrestrial samples by bulk fluorination of Ag_2S extracts (Farquhar et al., 2000). The anomalous fractionations have been validated by ion microprobe analyses (Mojzsis et al., 2001; Runnegar, 2001) and by repeated reanalysis (Farquhar et al., 2001c). The discovery has the potential for dramatic and far-reaching implications in understanding the history of the Earth's atmosphere (Kasting, 2001). The existence of a previously unrecognized geological record of the long-term evolution of the Earth's atmospheric chemistry may now be in hand (Farquhar et al., 2000). Much work needs to be done, however. Understanding the significance of mass-independently fractionated sulfur isotopes in Archean and Paleoproterozoic rocks requires locating and identifying the host minerals of anomalous sulfur. The geographic and stratigraphic distributions and variations of sulfur isotope anomalies must also be mapped and documented. The new UV laser sulfur isotope microprobe described herein is fully capable of making a major contribution to this effort because it provides in situ multisulfur isotope analyses of sulfide minerals.

Fluorination of sulfides to produce SF_6 for mass spectrometry with a CO_2 laser (Rumble et al., 1993; Beaudoin and Taylor, 1994) provides high precision and moderate spatial resolution for the analysis of sulfur isotopic compositions in sulfide minerals. Fluorine has only one stable isotope (^{19}F), which makes SF_6 an ideal analyte gas for measuring the $^{33}S/^{32}S$, $^{34}S/^{32}S$, and $^{36}S/^{32}S$ ratios. The use of SO_2 gas as analyte for measurements of $^{34}S/^{32}S$ is far more prevalent than the use of SF_6, but isobaric interferences by the three oxygen isotopes, ^{16}O-^{17}O-^{18}O, make its use for analyzing $^{33}S/^{32}S$ and $^{36}S/^{32}S$ problematic (Hulston and Thode, 1965; Rees, 1978). Rumble et al. (1993) demonstrated that direct in situ analyses of sphalerite, chalcopyrite, galena, and pyrite with a CO_2 laser probe provided comparable precision and accuracy to conventional bulk SO_2 or BrF_5-SF_6 methods. However, the possibility of mineral-specific fractionation effects cannot be ruled out. Laser craters made with a CO_2 laser in chalcopyrite exhibit alteration halos of bornite extending 80 μm radially outward from crater walls (Rumble et al., 1993). Furthermore, it is occasionally observed that the intense thermal shock imparted by a CO_2 laser to a mineral surface may crack the sample. This may be accompanied by possible spontaneous sulfur isotope fractionation (Beaudoin and Taylor, 1994).

The use of a UV laser proved to be crucial in obtaining high-precision, in situ, spot analyses of oxygen isotope ratios in silicate and oxide minerals (Wiechert and Hoefs, 1995; Rumble et al., 1997; Young et al., 1998; Fiebig et al., 1999). Photoablation with UV light in contrast to thermal ablation with infrared (IR) light is stoichiometric and yields unfractionated oxygen isotopes. Compared to an IR laser, a UV laser is likely to afford analytical advantages for sulfur isotope analyses, including smaller spot size, greater likelihood of stoichiometric ablation, and less dependence on an operator's skill. Good energy coupling between UV light and sulfides is expected on the basis of absorption spectroscopy measurements (Sato, 1984).

We have built a sulfur isotope laser microprobe incorporating photoablation with a KrF excimer laser; a choice of thermal ablation with a CO_2 laser; analyte purification with an automated gas chromatograph (GC); a water-cooled, corrosion-resistant, turbomolecular vacuum pump; and on-line fluorine purification (Fig. 1). Two lasers are required: one for the whole-grain analysis of mineral powders by IR heating and one for the in situ spot analysis of mineral surfaces by UV photoablation. The IR laser is a CO_2 laser ($\lambda = 10.6$ μm). The UV laser is an excimer laser that was chosen because its wavelength can be switched from $\lambda = 248$ nm to $\lambda = 193$ nm by changing the chemical composition of the gas in the resonance cavity. Analyses of powdered sulfides with a CO_2 laser play a crucial role in confirming the accuracy of in situ spot analysis with a KrF excimer laser. The accuracy of the analytical system was demonstrated by CO_2 laser fluorination of International Atomic Energy Agency (IAEA) and National Institute of Standards and Technology (NIST) isotope reference materials. The validity of in situ spot analyses of sulfides was demonstrated by comparing analyses of laser craters with powders from side-by-side drill holes. In situ spot analyses of sulfides with a KrF excimer laser ($\lambda = 248$ nm) provide results equal in precision and accuracy to those obtained by CO_2 laser analyses of powders from drill holes. There are no mineral specific fractionation effects.

2. INSTRUMENTATION

The laser microprobe system consists of four parts: laser, vacuum line, GC, and mass spectrometer. Diagrams of the vacuum line and GC systems are shown in Figures 1 to 3. The GC is on line to the mass spectrometer and the laser fluorination system. The reaction chamber used for the analysis of powdered sulfides with the CO_2 laser is the same as that of Sharp (1990). The reaction chamber for in situ analysis of sulfides in rock slabs with a KrF excimer laser has a single MgF_2 or UV-grade quartz window and is connected to the vacuum line by a flexible, bellows-type vacuum hose (Fig. 2; Rumble et al., 1997).

Two different lasers were used. The IR laser is a Synrad 25-W CO_2 laser ($\lambda = 10.6$ μm). The UV laser is a Lambda-Physik Compex model 110 excimer laser with beam delivery optics and automated sample positioning stage, as described by Rumble et al. (1997) and Farquhar and Rumble (1998). IR heating is required for analysis of powders. UV lasers cannot be used for analyzing powders because they violently disperse granular materials. The excimer laser wavelength can be changed in <1 h by filling the resonance cavity with either KrF ($\lambda = 248$ nm) or ArF ($\lambda = 193$ nm) gas mixtures. In this study, the spot size of the rectangular excimer laser beam for in situ analyses was typically 600×800 μm, with a crater depth of 600 μm. The minimum spot size is constrained not by the laser

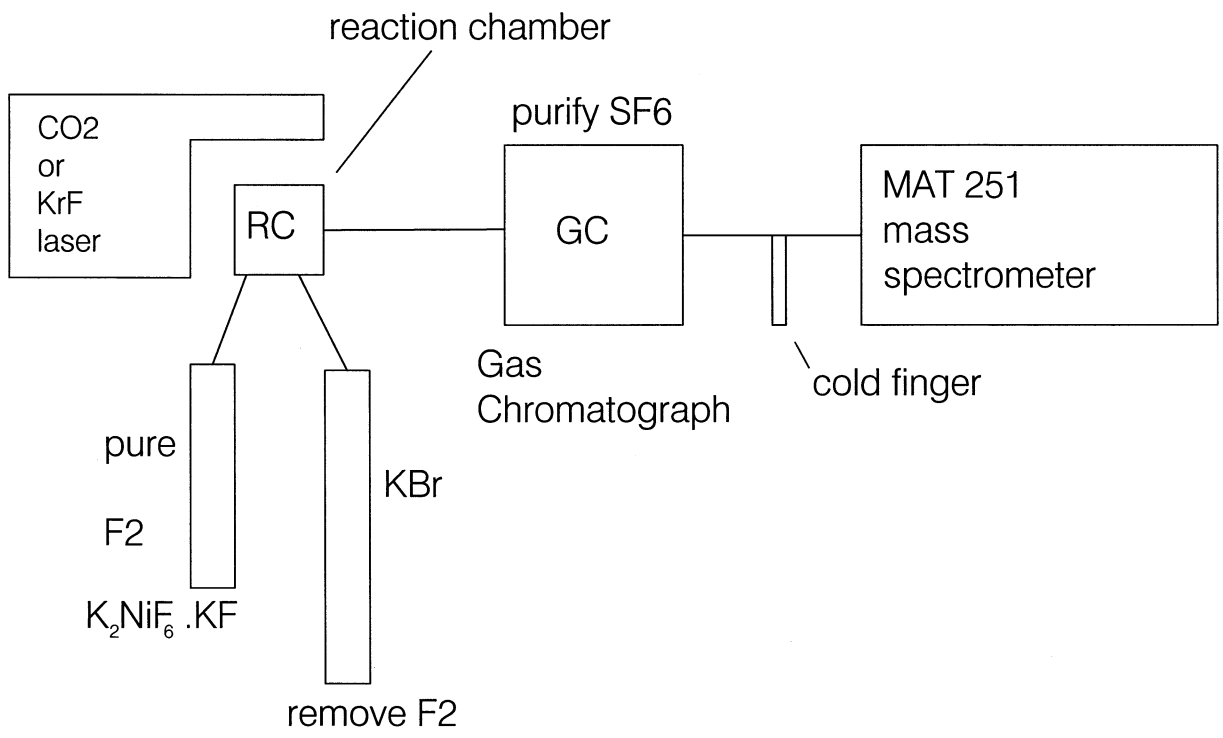

Fig. 1. Schematic diagram of KrF and CO_2 laser sulfur isotope analysis system.

system but by the requirement that sufficient SF_6 ($\geq$1 μmol) must be produced for mass spectrometer operation.

The GC is a Shimadzu GC-8AIT model equipped with dual 0.125-in outside diameter, 2-m columns (one for sample and one for reference) packed with Haysep Q substrate, 80 to 100 mesh (Fig. 3). A thermal conductivity detector (TCD) achieves high sensitivity with a bridge circuit for measuring the difference in conductivity between the sample-loaded and reference columns. The GC operates under computer control at 100°C with a helium carrier flow of 30 cm^3/min. The system is designed to operate with an isotope ratio–monitoring GC inlet mass spectrometer. Pending acquisition of the new instrument, the analyses reported herein were performed with a MAT 251 conventional dual-inlet mass spectrometer. The Finnigan-MAT 251 mass spectrometer is equipped with a quadruple collector assembly for simultaneous measurement of the ion beams at masses 127 ($^{32}SF_5^+$), 128 ($^{33}SF_5^+$), 129 ($^{34}SF_5^+$), and 131 ($^{36}SF_5^+$) (Rumble et al., 1993).

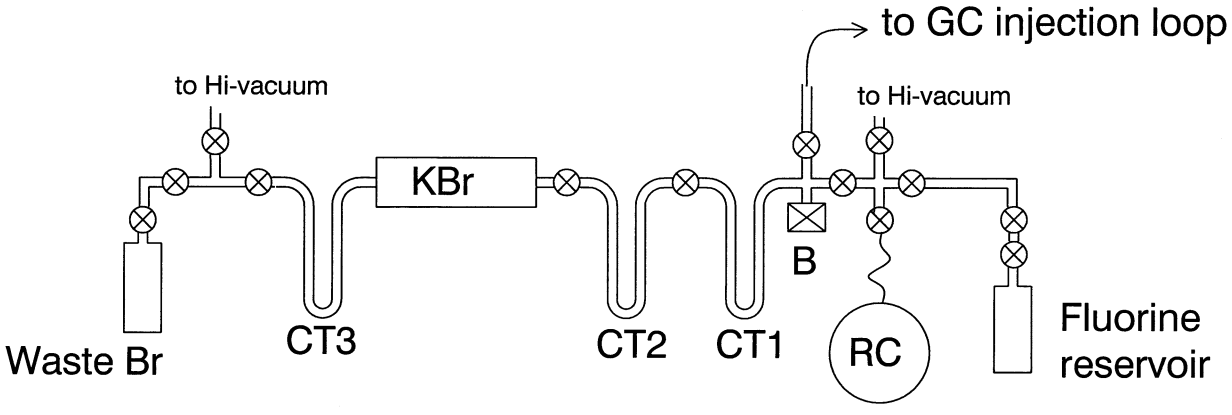

Fig. 2. Vacuum line for laser fluorination of sulfide minerals. Pure fluorine generated by heating K_2NiF_6●KF (Asprey, 1976). B = capacitance manometer; CT = liquid nitrogen cold trap; GC = gas chromatograph; RC = reaction chamber. CT1 with liquid nitrogen is open to RC throughout lasing. CT2 is used during passivation of F_2 over heated KBr to prevent back diffusion of Br_2 into CT1. CT3 is needed to complete passivation of F_2. Progress of fluorination reactions monitored on baratron B.

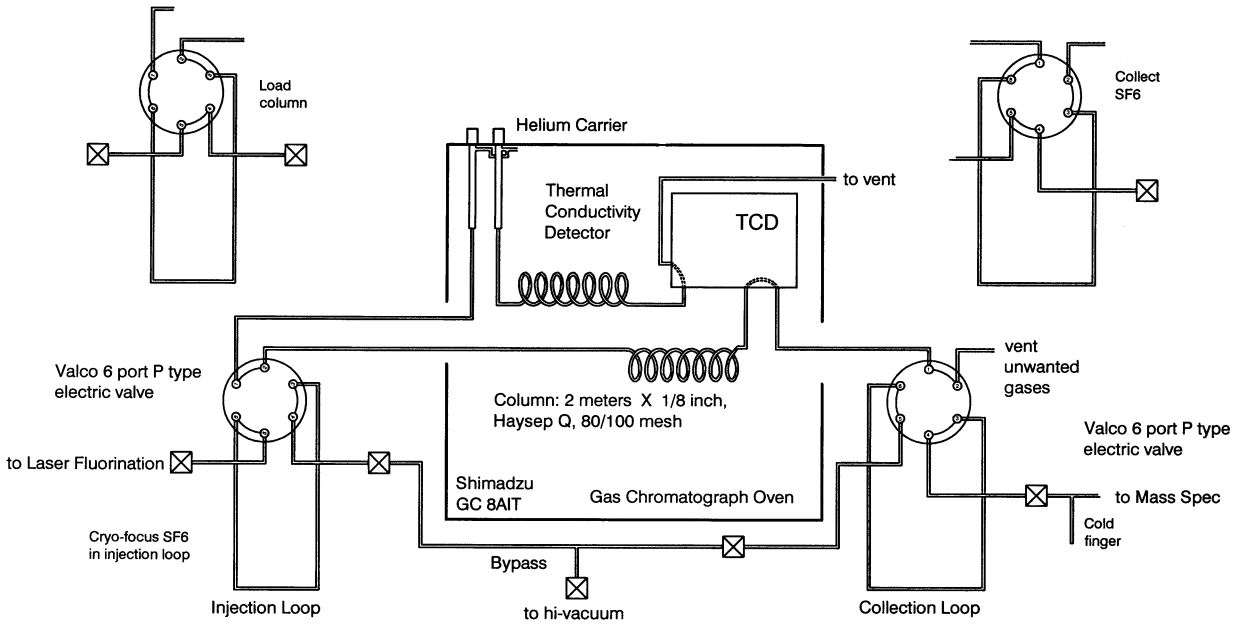

Fig. 3. Gas chromatograph (GC) for purification of SF_6. The two Valco valves are shown in both the "load" and "inject" positions.

3. ANALYTICAL PROCEDURE

3.1. Sample Preparation

Powdered samples were prepared by standard mineral separation techniques, by hand picking, or by drilling holes into mineral surfaces with diamond-tipped dentist's drills. Samples for in situ analysis were prepared by cutting chips of rocks or minerals into $0.5 \times 1 \times 2$ cm pieces. No oils, organic reagents, epoxies, or glues were used in preparing polished rock chips. Water is used to cool rock saw blades and to mix abrasive slurries for grinding and polishing. For making spot analysis of individual mineral grains, samples were placed into stainless steel (alloy 316) cups ~1 cm in diameter. The grains were fixed in the cups with small stainless steel set screws to prevent mineral grain movement under the laser beam. Polishing rock slabs is required to observe microstructures and mineral intergrowths, but spot analyses were completed successfully on unpolished mineral surfaces.

3.2. Spontaneous Fluorination

Candidate samples for in situ analysis typically experience spontaneous fluorination reactions when first exposed to fluorine in the reaction chamber. These reactions release gases such as HF and O_2. The phrase "spontaneous fluorination" is used to underscore the observation that such reactions occur before laser firing. In most cases, the reaction of fluorine with moisture adsorbed by the sample and on the walls of the reaction chamber is responsible for spontaneous reaction. Spontaneous fluorination of adsorbed H_2O is, by itself, not an obstacle to successful analysis because water can be eliminated by repeated heating, vacuum pumping, and prefluorination until no additional reaction is observed (Rumble et al., 1993; Beaudoin and Taylor, 1994). In some other cases, however, rock chips containing easily fluorinated minerals such as alkali feldspar, calcite, or clay minerals react spontaneously producing HF and O_2. These gases may react during lasing of sulfides, yielding in addition to SF_6 undesirable products such as SOF_2 and SO_2F_2 (Rumble et al., 1993; Beaudoin and Taylor, 1994). The generation of S-O-F gases may create analytical difficulties because the presence of more than one sulfur-bearing gas species causes sulfur isotope fractionation (see SF_6-SO_2F_2-SOF_2 fractionation factors calculated by Oi et al., 1985). In some cases, the minerals responsible for spontaneous fluorination can be eliminated by repeated prefluorination. These samples are viable candidates for in situ laser fluorination analysis. When prefluorination does not eliminate fluorine-susceptible minerals, the samples are unsuitable for in situ laser fluorination analysis (Rumble et al., 1993; Beaudoin and Taylor, 1994). The experience in our laboratory runs the gamut from clean, readily analyzed samples to those impossible to analyze. Among the most frustrating examples of impossible in situ samples are eclogite samples weathered in humid climates. These were impossible to analyze for oxygen isotopes. In the present study, it has been found that unweathered drill core samples of pyrite-bearing black shale are excellent subjects for in situ laser fluorination analysis of sulfur isotopes.

3.3. Prefluorination

In view of the dangers of spontaneous fluorination for in situ analysis, it is imperative that every sample be tested for fluorine susceptibility. Each sample behaves differently in fluorine, even samples collected from the same outcrop and those with identical in-hand specimen appearance. Samples must therefore be tested individually.

Spontaneous fluorination is measured for every sample by exposing the reaction chamber to 15 torr of fluorine previously

Table 1. Interlaboratory comparison of $\delta^{34}S_{V\text{-}CDT}$ values of reference materials measured with CO_2 laser.

Sample	$\delta^{34}S_{V\text{-}CDT}$, ‰[a]	$\delta^{34}S_{V\text{-}CDT}$, ‰ (MILES-$SF_6$)[b]	$\delta^{34}S_{V\text{-}CDT}$, ‰ ($BrF_5$-$SF_6$)[c]	$\delta^{34}S_{V\text{-}CDT}$, ‰ ($BrF_5$-$SF_6$)[d]	$\delta^{34}S_{V\text{-}CDT}$, ‰ ($SO_2$)[e]
IAEA-S-1	–0.3 (13, 0.2)	–0.3	–0.3	–0.3	–0.3
IAEA-S-2	+22.5 (12, 0.4)	+22.7	+22.7	22.6	+21.8
IAEA-S-3	–32.1 (10, 0.2)	–32.2	–32.6	–32.1	–31.6
NBS 123	+18.2 (6, 0.2)	+18.2	17.4		17.1

IAEA = International Atomic Energy Agency; MILES = Micro in situ laser extraction system; NBS = National Bureau of Standards.
[a] Geophysical Laboratory new CO_2 laser microprobe. Define IAEA-S-1 = −0.3‰. First number in the parentheses shows number of analyses; second number is 1σ standard deviation.
[b] Geological Survey of Canada MILES laser microprobe (Taylor, in press).
[c] Institute of Mineral Deposits, Chinese Academy of Sciences, Beijing, BrF_5-fluorination (Ding et al 2001).
[d] Institute for Reference Materials and Measurements, Geel, Belgium (Ding et al 2001).
[e] Running average of IAEA interlaboratory comparison (Taylor, in press).

equilibrated with a liquid nitrogen cold trap (CT 1, Fig. 2). Condensable reaction products of spontaneous fluorination such as SF_6, HF, SO_2F_2, and SOF_2 freeze into the cold trap (CT 1, Fig. 2), and pressure decreases are observed on an MKS Baratron capacitance manometer (baratron B, Fig. 2). The reaction is allowed to proceed until the pressure reaches a stationary value. Excess fluorine is passivated over heated KBr, the condensable gases are pumped away, and prefluorination is repeated. Typically, two to three prefluorination treatments are needed to eliminate spontaneous fluorination. The final test for spontaneous fluorination is to load F_2 previously equilibrated in the liquid nitrogen cold trap (CT 1, Fig. 2) into the reaction chamber and to verify that there is no change in pressure over a period of several minutes. If a decrease in pressure occurs, the sample is not ready for analysis, and prefluorination must be repeated. The SF_6 blank from a sample that shows no pressure change during prefluorination testing is below 0.05 μmol, as determined by gas chromatography. This is an amount too small to measure for isotope ratios on the MAT 251 mass spectrometer.

3.4. Analysis

Pure F_2 gas is generated with the method developed by Asprey (1976), as described by Rumble et al. (1993) (Figs. 1 and 2). Prefluorination of powders must be tested on a sample-by-sample basis because a number of minerals react spontaneously and completely and thus are lost. Fine-grained samples of troilite, sphalerite, chalcopyrite, pyrrhotite, and pyrite were prefluorinated successfully in this study, but powdered Ag_2S and galena fluorinated spontaneously and were loaded one at a time to avoid cross-contamination. Care should be taken in prefluorinating the very fine-grained powders obtained by drilling into mineral surfaces with a diamond-tipped drill because these are susceptible to spontaneous fluorination. Water is removed from these samples by combined heating and vacuum pumping. As an alternative to one-at-a-time loading, the analysis of powdered samples that spontaneously react with F_2 at room temperature may be carried out in a reaction chamber chilled with liquid nitrogen (B. E. Taylor, personal communication, 2001). Routine analysis of powders uses a CO_2 laser and follows the methods described by Rumble et al. (1993).

Table 2. Interlaboratory comparison of $\delta^{33}S_{V\text{-}CDT}$ values of reference materials measured with CO_2 laser. Values reported to two decimals to facilitate comparison to published data.

Sample	$\delta^{33}S_{V\text{-}CDT}$, ‰[a]	$\delta^{33}S_{V\text{-}CDT}$, ‰ ($BrF_5$-$SF_6$)[b]	$\delta^{33}S_{V\text{-}CDT}$, ‰ ($BrF_5$-$SF_6$)[c]
IAEA-S-1	–0.11 (13, 0.1)	–0.05	–0.05
IAEA-S-2	11.54 (12, 0.2)	11.48	11.65
IAEA-S-3	–16.60 (10, 0.1)	–16.65	–16.56

IAEA = International Atomic Energy Agency.
[a] Geophysical Laboratory SF_6 laser microprobe. First number in the parentheses shows number of analyses; second number is 1σ standard deviation.
[b] Institute of Mineral Deposits, Chinese Academy of Sciences, Beijing, BrF_5-fluorination (Ding et al 2001).
[c] Institute for Reference Materials and Measurements, Geel, Belgium (Ding et al 2001).

For in situ spot analysis of sulfides with the KrF excimer laser, samples were out-gassed under vacuum and prefluorinated three times with 15 torr F_2 for 10 min each before analysis. Approximately 20 torr of F_2 gas previously equilibrated with liquid nitrogen in cold trap 1 (Fig. 2) was expanded into the reaction chamber to begin an analysis. The laser operating conditions were adjusted to deliver a fluence of 7 to 13 J/cm^2 at the sample surface. The laser was fired 2000 to 10,000 times at 10 to 20 shots per second to acquire enough SF_6 ($\geq$1 μmol) for mass spectrometry. The generated SF_6 was condensed into the liquid nitrogen trap (CT 1, Fig. 2) next to the reaction chamber as it formed during fluorination. The decrease in pressure monitored on baratron B throughout lasing measures the progress of fluorination as SF_6 condenses into cold trap 1 (Fig. 2). It is important to remove SF_6 as rapidly as possible from the laser beam by condensation into a cold trap to avoid photochemical isotope fractionation (cf. discussion of isotope fractionation by CO_2 laser in Rumble et al., 1993; Beaudoin and Taylor, 1994).

After completion of fluorination, excess F_2 was neutralized by reaction with heated KBr (Figs. 1 and 2). SF_6 and trace amounts of C-O-F-S compounds remaining in the cold trap were thawed. The mixture was frozen with liquid nitrogen into the injection loop of the GC (Fig. 3). Helium gas was introduced into the thawed injection loop to carry the mixture through the GC column. SF_6 was separated from unwanted contaminants on the GC column. The gas flow was routed through a liquid nitrogen collection loop immediately after the SF_6 peak emerged from the TCD (Fig. 3). After the SF_6 eluted

Table 3. Mass-dependent sulfur isotope fractionation measured with KrF and CO_2 lasers.

Sample	Laser	$\delta^{33}S$ ‰[a]	$\delta^{34}S$ ‰[b]	$\Delta^{33}S$ ‰
Canon Diablo troilite	KrF	0.0 (11,0.1)	0.2 (0.2)	–0.07
IAEA-S-1 (Ag_2S)	CO_2	–0.1 (13,0.1)	–0.3 (0.2)	0.04
IAEA-S-2 (Ag_2S)	CO_2	11.5 (12,0.2)	22.5 (0.4)	–0.06
IAEA-S-3 (Ag_2S)	CO_2	–16.6 (10,0.1)	–32.1 (0.2)	–0.05
NBS 123 sphalerite	CO_2	9.3 (6, 0.1)	18.2 (0.2)	–0.07
Broken Hill sphalerite (in situ)	CO_2[c]	2.0	4.0	–0.06
	CO_2[c]	1.9	3.8	–0.06
	KrF	2.0	4.0	–0.06
	KrF	2.1	4.1	–0.01
	KrF	1.8	3.7	–0.11
	KrF	2.0	3.9	–0.01
	KrF	1.9	3.8	–0.06
	KrF	1.8	3.7	–0.11
Pyrite 1	CO_2	–16.7 (5, 0.1)	–32.3 (0.2)	–0.07
Pyrite 2	CO_2	15.2 (4, 0.2)	29.7 (0.4)	–0.10
Pyrite-M (in situ)	CO_2[c]	1.9	3.7	–0.01
	CO_2[c]	2.1	4.0	0.04
	CO_2[c]	2.1	4.1	–0.01
	CO_2[c]	2.7	5.3	–0.03
	CO_2[c]	2.4	4.7	–0.02
	CO_2[c]	2.6	5.0	0.02
	KrF	1.9	3.7	–0.01
	KrF	2.7	5.3	–0.03
	KrF	2.9	5.6	0.02
	KrF	2.7	5.3	–0.03
	KrF	2.7	5.4	–0.08
	KrF	2.9	5.7	–0.04
	KrF	2.7	5.6	–0.18
	KrF	2.3	4.5	–0.02
Galena (in situ)	CO_2[c]	–3.5	–6.8	0.00
	CO_2[c]	–4.1	–7.7	–0.13
	CO_2[c]	–3.9	–7.6	0.01
	CO_2[c]	–4.0	–7.5	–0.14
	CO_2[c]	–3.5	–6.7	–0.05
	CO_2[c]	–2.8	–5.6	0.08
	KrF	–3.5	–6.8	0.00
	KrF	–3.8	–7.4	0.01
	KrF	–3.8	–7.4	0.01
	KrF	–3.8	–7.3	–0.04
	KrF	–3.7	–7.4	0.11
	KrF	–3.8	–7.4	0.01
	KrF	–3.7	–7.3	0.06
Chalcopyrite (in situ)	CO_2[c]	5.2	10.1	0.00
	CO_2[c]	4.4	8.5	0.02
	CO_2[c]	4.7	9.2	–0.04
	CO_2[c]	4.4	8.7	–0.08
	KrF	4.8	9.4	–0.04
	KrF	4.5	8.7	0.02

IAEA = International Atomic Energy Agency; NBS = National Bureau of Standards.

[a] First number in parenthesis is number of analyses; second number is 1σ.

[b] Number in parenthesis is 1σ.

[c] Drill hole sample.

and was frozen in the collection loop, helium flow was vented into a fume hood to dispose of unwanted contaminants. The amount of SF_6 was determined by measuring its peak area with a calibrated GC TCD. Helium carrier gas was pumped away very slowly through the bypass (Fig. 3) while the collection loop was still frozen. The purified SF_6 was expanded into the mass spectrometer for analysis via a cold finger (Fig. 3). The total process for analyzing one sample takes ~45 min. The following data are from analyses of SF_6 purified by one pass through the GC. A single purification pass is sufficient to obtain accurate and precise $\delta^{34}S_{V\text{-}CDT}$ and $\delta^{33}S_{V\text{-}CDT}$ values (Rumble et al., 1993, Table 1, p. 4503). Multiple GC purification is required to obtain accurate $\delta^{36}S$ values (Gao and Thiemens, 1991). Although we measured $\delta^{36}S$, it is not reported here because we did not take the extra time necessary to achieve adequate purification.

4. INTERLABORATORY REFERENCE MATERIALS

4.1. Mass Spectrometer Notation

The results of sulfur isotopic analyses are reported in "delta" notation with units of per mil (‰), where

$$\delta^{34}S_{V\text{-}CDT} = [(^{34}S/^{32}S)_{sample}/(^{34}S/^{32}S)_{V\text{-}CDT}-1] \times 1000.$$

The subscript "V-CDT" refers to the IAEA sulfur isotope reference standard IAEA-S-1 (Ag_2S), with $\delta^{34}S_{V\text{-}CDT}$ defined as – 0.3‰ (Coplen and Krouse, 1998). $\delta^{33}S_{V\text{-}CDT}$ is defined as

$$\delta^{33}S_{V\text{-}CDT} = [(^{33}S/^{32}S)_{sample}/(^{33}S/^{32}S)_{V\text{-}CDT}-1] \times 1000,$$

with $\delta^{33}S_{V\text{-}CDT} = -0.1$‰, as measured in this laboratory.

Analytical uncertainties are reported as $\pm 1\sigma$. The reported precision is external precision, i.e., the standard deviation of either replicate analyses of different aliquots of the same powdered sample or replicate analyses of different laser craters in the same sulfide sample. Repeated laser fluorination of IAEA-S-1 shows that our mass spectrometer working standard SF_6 has $\delta^{34}S_{V\text{-}CDT} = +0.2 \pm 0.1$‰ and $\delta^{33}S_{V\text{-}CDT} = +0.1 \pm 0.1$‰.

The quantity $\Delta^{33}S$ is defined as $\Delta^{33}S = \delta^{33}S - 0.515 \times \delta^{34}S$ ‰, approximately. In the text and tables, $\delta^{34}S$ and $\delta^{33}S$ values are rounded and reported to the first decimal. Values of $\Delta^{33}S$ are reported to the second decimal. The $\Delta^{33}S$ values were calculated with two decimal values of $\delta^{34}S$ and $\delta^{33}S$, as reported by the mass spectrometer data system.

4.2. Interlaboratory Comparison of Powdered Reference Materials

The accuracy of the laser analytical system was established by analyzing four powdered interlaboratory reference materials with a CO_2 laser, including National Bureau of Standards (NBS) 123 (sphalerite) and three IAEA Ag_2S standards: IAEA-S-1 (previously identified as NZ-1), IAEA-S-2 (previously identified as NZ-2), and IAEA-S-3 (Ding et al., 2001). The results are shown in Tables 1 and 2. The yields of SF_6 for NBS 123 are from 70 to 100%. Low yield occurred when mineral grains jumped out of the sample holder. The isotopic compositions of replicate analyses of NBS 123 do not change with yield. The yield of IAEA Ag_2S samples varied from 58 to 94%. No change of isotopic value with yield of Ag_2S sample was observed.

The $\delta^{34}S_{V\text{-}CDT}$ values of sulfur isotope reference materials measured at the Geophysical Laboratory (Tables 1 and 2) agree within 0.2‰ with the results obtained by the MILES laser fluorination technique (Beaudoin and Taylor, 1994), within 0.2 to 0.8‰ with the externally heated BrF_5-SF_6 method (Ding et al., 2001), and within 0.5 to 1.0‰ with the SO_2 method (Taylor

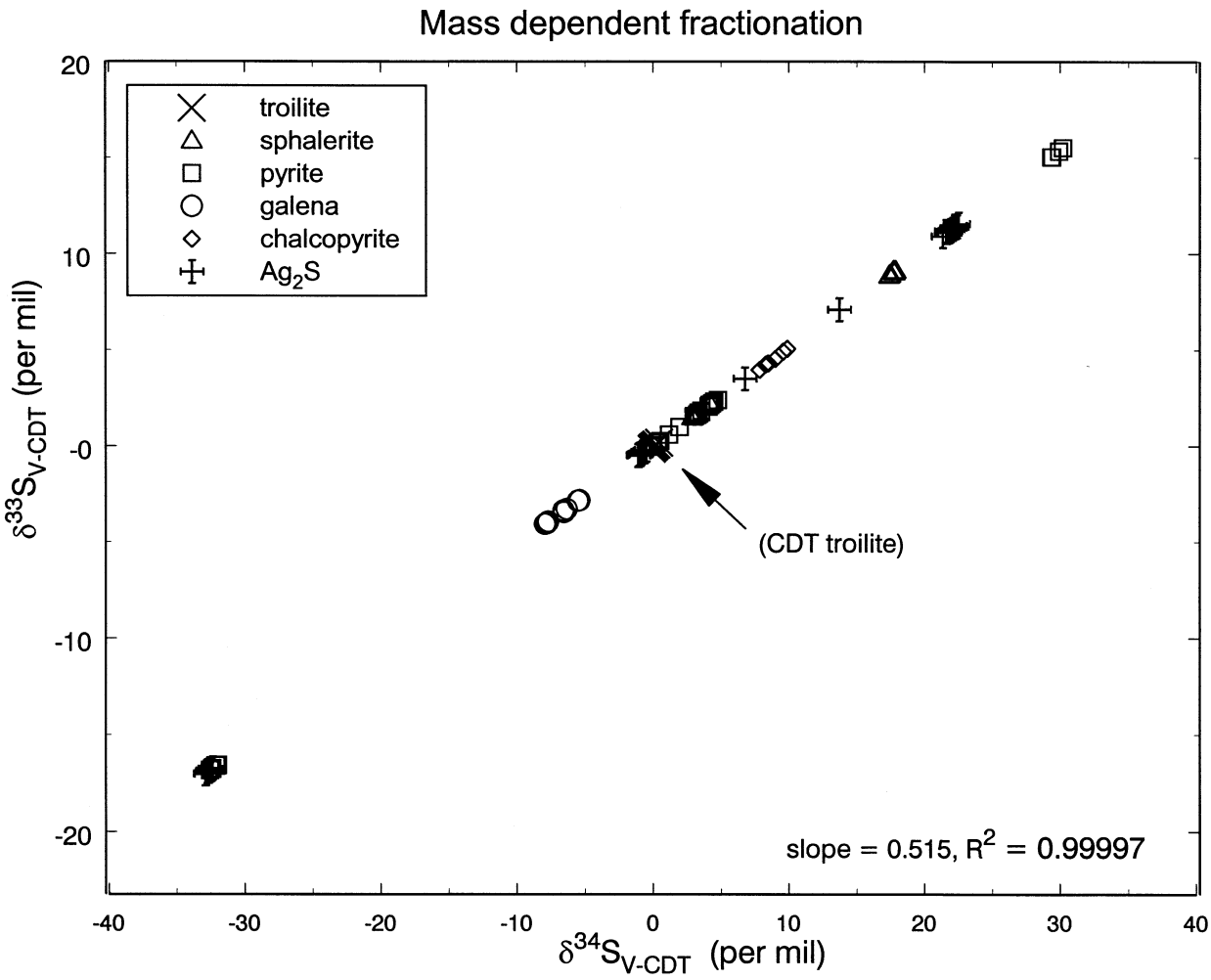

Fig. 4. $\delta^{34}S_{V\text{-}CDT}$ vs. $\delta^{33}S_{V\text{-}CDT}$ for KrF and CO_2 laser analyses. Analyses follow locus of mass-dependent fractionation.

et al 2003). The relatively large differences between our results and the results of the SO_2 method may be attributed to the systematic discrepancies between the SF_6 method and the SO_2 method discussed by Rees (1978), Beaudoin and Taylor (1994), and Taylor (in press).

The $\delta^{33}S_{V\text{-}CDT}$ values of sulfur isotope reference materials measured at the Geophysical Laboratory (Table 2) agree within ± 0.1‰ with measurements made by SF_6-BrF_5 bulk fluorination (Ding et al., 2001).

4.3. Mass-Dependent Fractionation of $\delta^{34}S_{V\text{-}CDT}$ and $\delta^{33}S_{V\text{-}CDT}$ in Interlaboratory Reference Materials

One of the objectives of constructing a new laser microprobe is to analyze multisulfur isotopes with high accuracy and precision to assess departures from mass-dependent isotope fractionation. An assessment of the validity of this analytical system may be made by showing that consistent values of $\delta^{34}S_{V\text{-}CDT}$ and $\delta^{33}S_{V\text{-}CDT}$ with $\Delta^{33}S = 0.00$ are obtained from samples unaffected by nuclear or photochemical processes (Table 3). An immediate difficulty is that such samples cannot be definitively identified a priori. Given a working assumption that the bulk Earth and meteorites have the same value of $\Delta^{33}S = 0.00$, one should be able to find reference samples for testing, however. Fortunately, the isotope reference materials available from IAEA and NIST as well as Phanerozoic igneous and hydrothermal samples examined to date are consistent with this assumption. It is recognized that circular reasoning is highly undesirable in matters of standardization and calibration. The assumption that bulk Earth has $\Delta^{33}S = 0.00$ will, it is hoped, be tested repeatedly with each new multi-isotope study of sulfur geochemistry. Shown in Figure 4 is a $\delta^{34}S_{V\text{-}CDT}$ vs. $\delta^{33}S_{V\text{-}CDT}$ mass-dependent fractionation line measured with the new KrF and CO_2 laser microprobe on sulfide minerals and Ag_2S extending over a range of $\delta^{34}S_{V\text{-}CDT} > 60$‰ (Table 3). The slope of a straight line fit through the origin and the data is 0.515 ($R^2 = 0.99997$). Some 109 analyses give an average for $\Delta^{33}S = -0.03 \pm 0.07$‰ (Fig. 4). Hulston and Thode (1965) gave a theoretical slope of 0.514. Strictly speaking, this slope depends on the reduced mass of specific molecules and thus varies with different sulfur species. Bains-Sahota and Thiemens (1988)

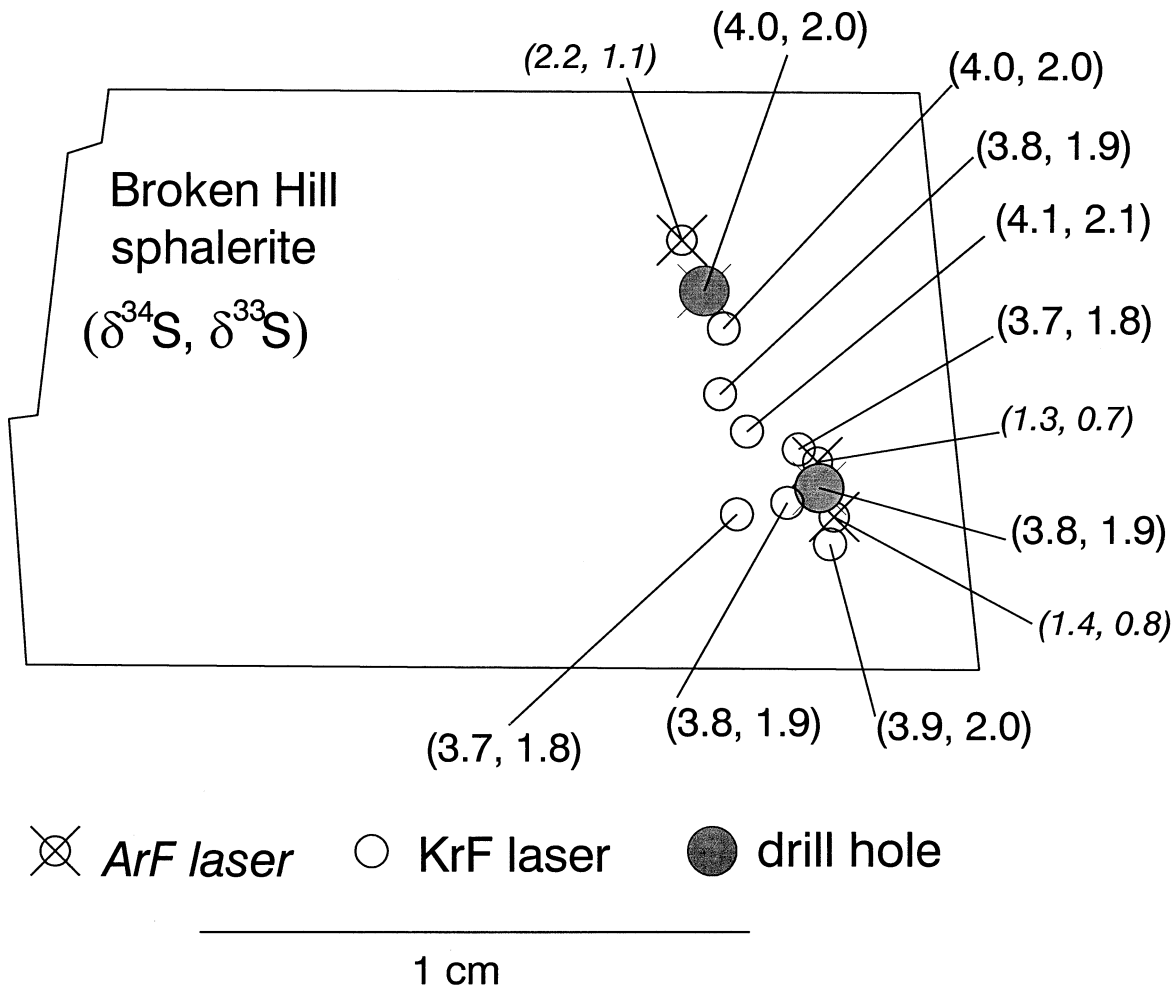

Fig. 5. In situ analyses of Broken Hill sphalerite. First number in parentheses is $\delta^{34}S_{V\text{-}CDT}$ value; second number is $\delta^{33}S_{V\text{-}CDT}$ value. Drill hole powders analyzed by CO_2 laser. Note agreement between drill hole and KrF excimer laser craters and disagreement between drill hole and ArF excimer laser craters.

measured $\delta^{33}S/\delta^{34}S$ ratios ranging from 0.501 to 0.518. A slope of 0.513 was previously measured in the Geophysical Laboratory (Rumble et al., 1993). The slope of the measured mass-dependent fractionation line and its zero value of mean $\Delta^{33}S$ establishes a datum against which mass-independent fractionations can be measured.

5. IN SITU ANALYSIS WITH UV LASER

5.1. Laser Craters

In situ analyses with a KrF excimer laser were tested on pyrite, sphalerite, galena, troilite, and chalcopyrite. Most of the craters measure 600 × 800 μm and are 600 μm deep with a flat bottom and steep sides. The fluoride products of KrF excimer laser fluorination are dispersed as a thin powdery blanket over the whole surface of the sample during lasing and are sulfur free (electron microprobe detection limit 1.0 wt.%). Rumble et al. (1993) observed that craters produced with a CO_2 laser were coated with metal fluorides and were surrounded by raised rims and ejecta blankets. UV laser craters are free from fluoride coating and encircling; raised rims were not observed.

Differences in the morphologies of KrF excimer laser craters and CO_2 laser craters may reflect differences in their fluorination mechanisms (Farquhar and Rumble, 1998). The metal-fluoride products of CO_2 laser fluorination remain mainly in the place where they form. The more vigorous fluorination of photoablation with a KrF excimer laser explosively generates a bright, blue to purple fluorescent plume of ionic, atomic, and molecular species and micrometer-sized particles. Metal-fluoride reaction products are dispersed throughout the reaction chamber and may deposit on the inside of the window, obscuring the view of the sample.

No sulfur-deficient halos or chemically altered rims were observed surrounding KrF excimer laser craters. A chemical profile across chalcopyrite measured from the crater wall radially outward with an electron microprobe analyzer shows that the mineral remains stoichiometric in Cu, Fe, and S (±0.5 wt.%) over a distance of 270 μm from the edge of the crater. There is no chemically altered host phase for fractionated

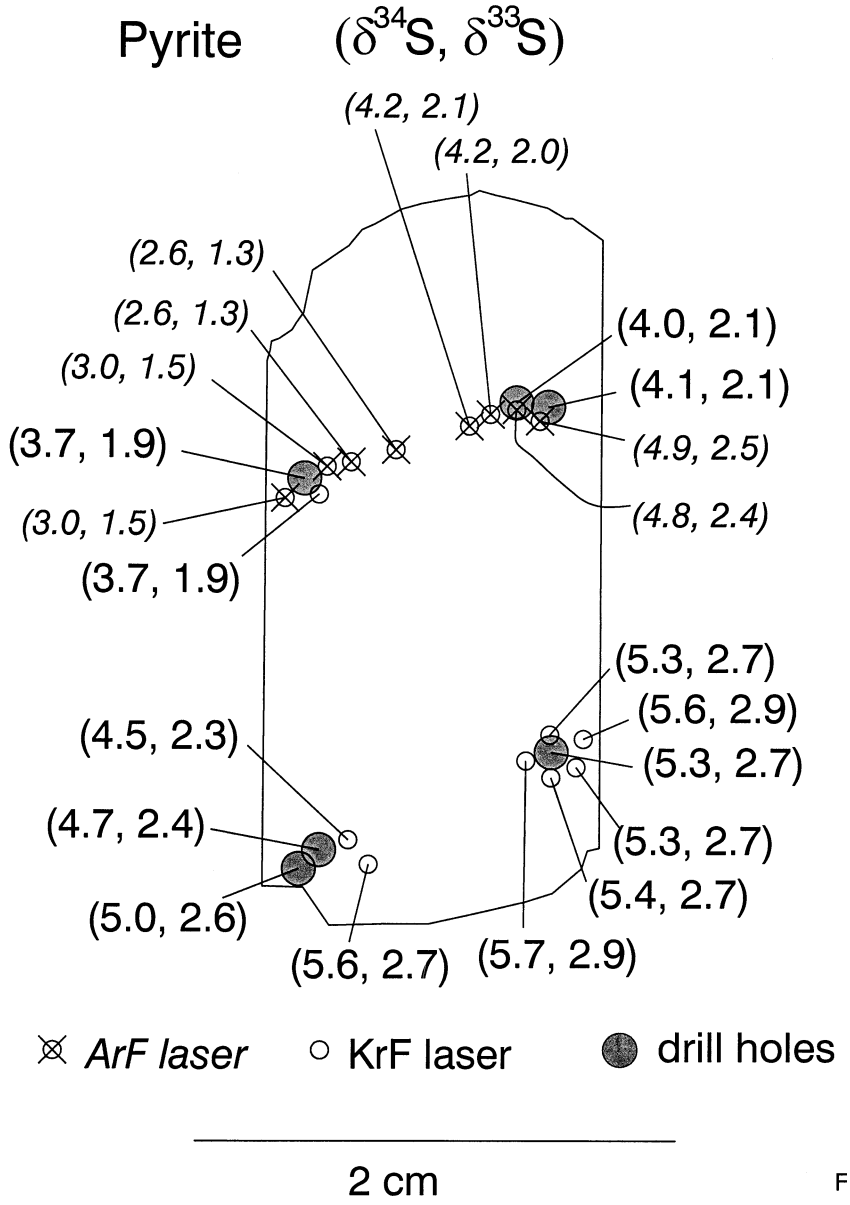

Fig. 6. In situ analyses of pyrite. First number in parentheses is $\delta^{34}S_{V\text{-}CDT}$ value; second number is $\delta^{33}S_{V\text{-}CDT}$ value. Drill hole powders analyzed by CO_2 laser. Note agreement between drill hole and KrF excimer laser craters and disagreement between drill hole and ArF excimer laser craters.

sulfur, in contrast to the bornite reaction rims reported by Rumble et al. (1993) for CO_2 laser craters in chalcopyrite. Therefore, crater rim fractionation is not a significant source of error for the in situ analysis of sulfur isotopes with a KrF excimer laser.

5.2. Accuracy and Precision

In situ analyses by KrF excimer laser were evaluated by comparison to CO_2 laser analyses of powders drilled at distances of 0.5 to 1 mm from laser craters. Analyses of granular sulfides made with a CO_2 laser have a precision and accuracy of $\pm 0.2‰$ for $\delta^{34}S$ and $\pm 0.1‰$ for $\delta^{33}S$, as measured on interlaboratory reference materials (Tables 1 and 2) (cf. Rumble et al., 1993; Beaudoin and Taylor, 1994). If the KrF excimer laser results agreed with CO_2 laser analyses within $\pm 0.2‰$ for $\delta^{34}S$ and $\pm 0.1‰$ for $\delta^{33}S$, this was accepted as satisfactory validation of the accuracy of spot analyses. We found acceptable accuracy for in situ spot analyses of sphalerite, pyrite, galena, and chalcopyrite with a KrF excimer laser. The data presented below demonstrate that in situ spot analyses of sphalerite, pyrite, galena, and chalcopyrite may be made with an accuracy of $\pm 0.2‰$ in both $\delta^{34}S$ and $\delta^{33}S$ with a KrF excimer laser. Spot analyses with an ArF excimer laser are fractionated in relation to whole-grain analyses with a CO_2 laser.

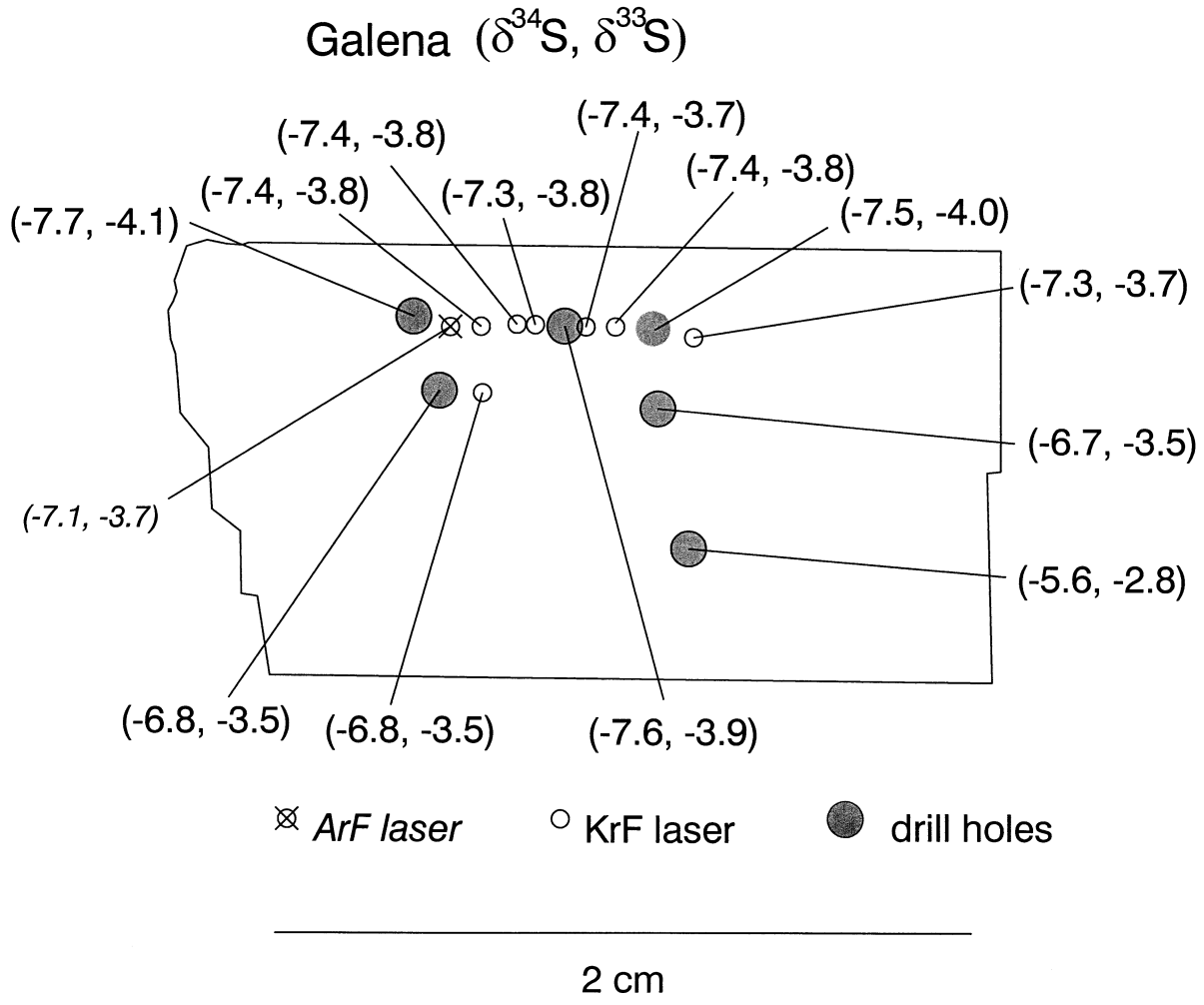

Fig. 7. In situ analyses of galena. First number in parentheses is $\delta^{34}S_{V\text{-}CDT}$ value; second number is $\delta^{33}S_{V\text{-}CDT}$ value. Drill hole powders analyzed by CO_2 laser. Note agreement between drill hole and KrF excimer laser craters and disagreement between drill hole and ArF excimer laser craters.

The sulfide minerals chosen for testing in situ analysis with a KrF laser include Broken Hill sphalerite (shown to be homogeneous by Rumble et al., 1993), an inhomogeneous galena (Rumble et al., 1993), pyrite, and chalcopyrite. The homogeneous sphalerite tests showed identical results for both an in situ KrF laser and analyses of drill hole powders with a CO_2 laser. The laser probe was built to analyze inhomogeneous minerals. The inhomogeneous samples provided a realistic test of how well the instrument does the job for which it was designed.

5.3. Results of in Situ Analysis

5.3.1. Sphalerite

The results of in situ spot analysis of sphalerite with a KrF excimer laser, an ArF excimer laser, and by CO_2 laser analysis of drill hole powders are shown in Figure 5 (Table 3). The gem-quality sphalerite sample is from an amphibolite-facies, metamorphosed deposit at Broken Hill, Australia. It was supplied by C. S. Eldridge (Australian National University) as an isotopically homogeneous mineral determined by ion microprobe (Rumble et al., 1993). The $\delta^{34}S_{V\text{-}CDT}$ values of powders from two drill holes 5 mm apart differ by 0.2‰, as measured by a CO_2 laser. Immediately adjacent spot analyses with a KrF excimer laser are identical for one drill hole with $\delta^{34}S = 4.0$‰ and $\delta^{33}S = 2.0$‰. In a second case, three KrF excimer laser analyses surrounding a drill hole average $\delta^{34}S = 3.8 \pm 0.1$‰ and $\delta^{33}S = 1.9 \pm 0.1$‰ compared to the drill hole with $\delta^{34}S = 3.8$‰ and $\delta^{33}S = 1.9$‰.

In situ spot analyses of sphalerite with an ArF excimer laser give $\delta^{34}S_{V\text{-}CDT}$ values differing by 1.8 to 2.5‰ in relation to CO_2 laser analyses of drill hole powders.

5.3.2. Pyrite

The results of in situ spot analyses of pyrite with a KrF excimer laser, an ArF excimer laser, and CO_2 laser analyses of drill hole powders are shown in Figure 6 (Table 3). CO_2 laser analysis of drill hole powders and KrF excimer laser spot analyses separated by 1 mm are identical at $\delta^{34}S = 3.7$‰ and

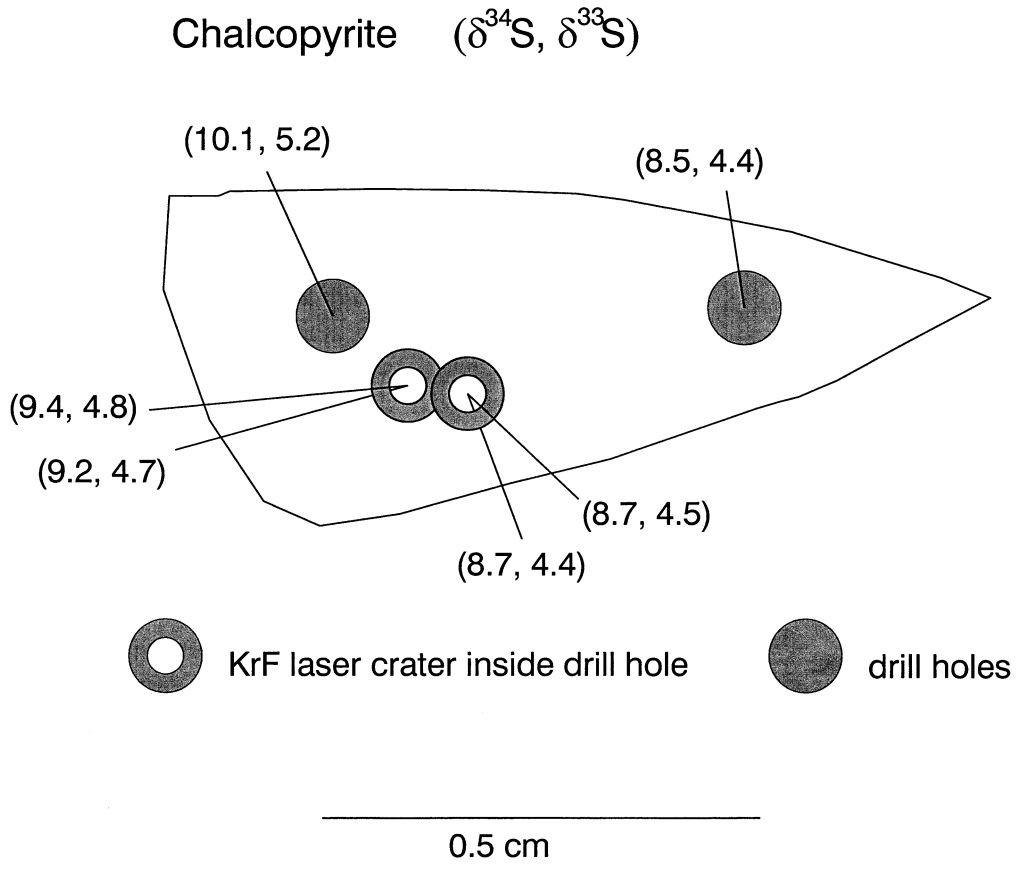

Fig. 8. In situ analyses of chalcopyrite. First number in parentheses is $\delta^{34}S_{V\text{-}CDT}$ value; second number is $\delta^{33}S_{V\text{-}CDT}$ value. Drill hole powders analyzed by CO_2 laser. Note agreement between drill hole and KrF excimer laser craters.

$\delta^{33}S = 1.9‰$. In a different area of the same mineral grain, a drill hole surrounded by five KrF excimer laser spot analyses gives $\delta^{34}S = 5.3‰$ and $\delta^{33}S = 2.7‰$ for CO_2 laser compared to an average of $\delta^{34}S = 5.5 \pm 0.2‰$ and $\delta^{33}S = 2.8 \pm 0.1‰$ for KrF excimer laser analyses (Fig. 6). A third area of the same mineral shows poorer agreement between drill hole powders and spot analyses, with CO_2 laser values of $\delta^{34}S = 4.7$ and 5.0‰ and $\delta^{33}S = 2.4$ and 2.6‰ and KrF excimer laser results of $\delta^{34}S = 4.5$ and 5.6‰ and $\delta^{33}S = 2.3$ and 2.7‰.

The differences between ArF excimer laser craters and adjacent CO_2 laser analysis of drill hole powders vary from −0.8 to +0.9‰ in $\delta^{34}S$.

5.3.3. Galena

In situ spot analyses of galena with ArF and KrF excimer lasers were tested with a galena sample previously analyzed by Rumble et al. (1993). Comparison between seven KrF excimer laser spot analyses and four adjacent CO_2 laser analyses of drill hole powders show close agreement (Fig. 7, Table 3). In one case, a KrF excimer laser analysis with $\delta^{34}S = -6.8‰$ and $\delta^{33}S = -3.5‰$ is identical to a drill hole located 1 mm distant, with CO_2 laser analysis of $\delta^{34}S = -6.8‰$ and $\delta^{33}S = -3.5‰$. In other areas of the galena grain, adjacent KrF excimer and CO_2 laser $\delta^{34}S$ values differ by 0.1 to 0.3‰.

A single-spot analysis by ArF excimer laser gives $\delta^{34}S = -7.1‰$ and $\delta^{33}S = -3.7‰$, with an adjacent CO_2 laser analysis of $\delta^{34}S = -7.7‰$ and $\delta^{33}S = -4.1‰$.

5.3.4. Chalcopyrite

To minimize the influence of chalcopyrite heterogeneity on the determination of the accuracy of in situ spot analysis, a KrF excimer laser was fired into the bottom of the drill holes sampled for CO_2 laser analysis (Fig. 8, Table 3). Pairs of CO_2 laser and KrF excimer laser analyses give $\delta^{34}S = 9.2‰$ and $\delta^{33}S = 4.7‰$ compared to $\delta^{34}S = 9.4‰$ and $\delta^{33}S = 4.8‰$ and a second pair with $\delta^{34}S = 8.7‰$ and $\delta^{33}S = 4.4‰$ compared to $\delta^{34}S = 8.7‰$ and $\delta^{33}S = 4.5‰$.

6. ASSESSING IN SITU ANALYSIS ERRORS

6.1. Errors in Aiming Laser

Accurate in situ analysis is critically dependent upon aiming the laser beam at the desired target, and this in turn depends on careful documentation of sample petrography before analysis. Test analyses show that overlapping the laser beam from target sulfides to adjacent silicates can result in large errors in $\delta^{34}S$ and $\delta^{33}S$ (Fig. 9). In situ analyses of a pyrite grain in an Archean quartz-biotite gneiss from Isua, Greenland, gave two pure pyrite analyses of $\delta^{34}S = 0.8‰$ and $\delta^{33}S = -0.5‰$ and

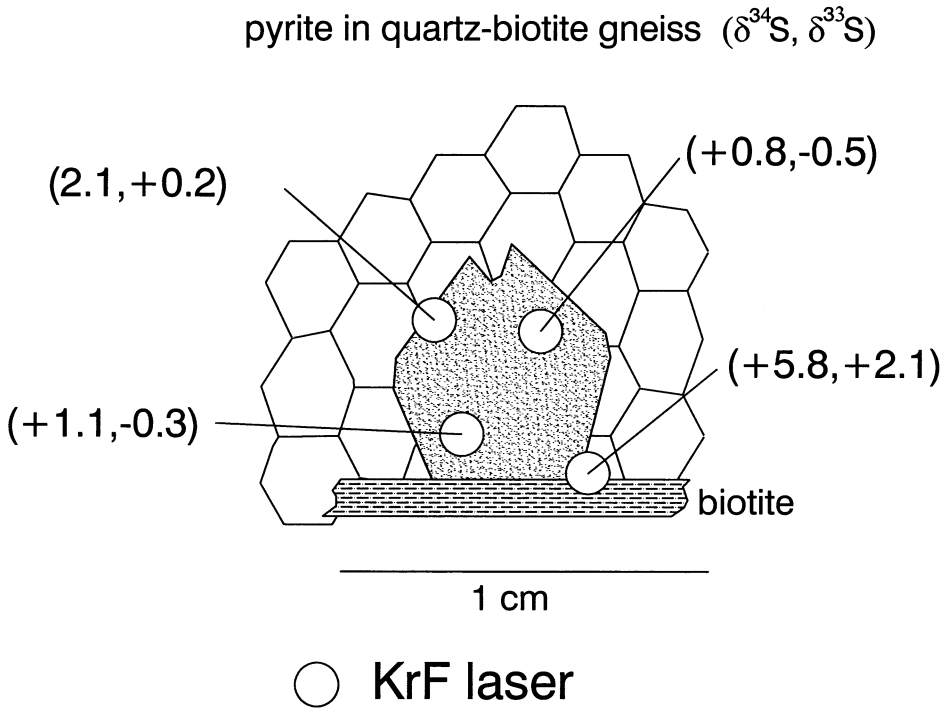

Fig. 9. KrF laser in situ analyses of pyrite in 3.8 Ga quartz-biotite gneiss, Isua, Greenland. Laser craters overlapping surrounding silicate minerals give variable $\delta^{34}S_{V\text{-}CDT}$ values, but $\Delta^{33}S_{V\text{-}CDT}$ values are identical to those of pyrite-only analyses (Table 5). (Sample from M. Rosing; analyst G. Hu).

$\delta^{34}S = 1.1‰$ and $\delta^{33}S = -0.3‰$, with $\Delta^{33}S = -0.87$ and $-0.84‰$, respectively. Allowing the laser beam deliberately to overlap a pyrite-biotite-quartz grain boundary resulted in $\delta^{34}S = 5.8‰$ and $\delta^{33}S = 2.1‰$; a pyrite-quartz grain boundary gives $\delta^{34}S = 2.1‰$ and $\delta^{33}S = 0.2‰$. The fractionated values of $\delta^{34}S$ and $\delta^{33}S$ arise because of partitioning of sulfur isotopes between SF_6 and the two gas species SO_2F_2 and SOF_2, which form when O_2 is released by fluorinating silicates in the presence of sulfides (Rumble et al., 1993; cf. Oi et al., 1985). Interestingly, the $\Delta^{33}S$ values of the pyrite-quartz and pyrite-biotite grain boundaries, -0.85 and $-0.86‰$, respectively, are identical to the two pure pyrite values within analytical precision (Table 5). The systematic behavior of $\Delta^{33}S$ values despite an overlapping laser beam illustrates an important point. The partitioning of ^{32}S, ^{33}S, and ^{34}S between different S-bearing species during laser fluorination is mass dependent and thus preserves a mass-independent fractionation signature (cf. secondary equilibration arrays for ^{16}O-^{17}O-^{18}O, Clayton and Mayeda, 1996).

6.2. Control of Laser Energy Fluence on $\delta^{34}S_{V\text{-}CDT}$ and $\Delta^{33}S$

The use of lasers in multi-isotope analyses has been a matter of concern because of separation of isotopes in excited ionic species or molecules (i.e., Lyman et al., 1975; Letokhov, 1979). Below, we review laser isotope fractionation and explain a technique for eliminating its effects. Selective dissociation of $^{32}SF_6$ isotopemers in a CO_2 laser beam causes $^{34}S/^{32}S$ and $^{36}S/^{32}S$ ratios of the remaining SF_6 gas to increase by 1000-fold compared to those of SF_6 gas before irradiation (Lyman et al., 1975; Letokhov, 1979). Nevertheless, results of measurements of reference materials in Tables 1 and 2 show no measurable selective laser isotope separation during fluorination of sulfides with the CO_2 laser probe (Table 3).

UV light is known to activate mass-independent fractionation effects for ^{16}O-^{17}O-^{18}O (e.g., Thiemens, 1999) and ^{32}S-^{33}S-^{34}S-^{36}S (Zmolek et al., 1999; Farquhar et al., 2001a) between certain gas molecules. Figure 10 shows the relation between the energy fluence of a KrF excimer laser at 248 nm and $\delta^{34}S_{V\text{-}CDT}$ and $\Delta^{33}S_{V\text{-}CDT}$. No dependence between laser energy fluence and $\delta^{34}S_{V\text{-}CDT}$ was observed. The $\Delta^{33}S_{V\text{-}CDT}$ values of the KrF excimer laser analyses of Phanerozoic hydrothermal and igneous sulfides are $0 \pm 0.07‰$.

No measurable laser isotope separation effect has been found with either the CO_2 or the KrF excimer laser in this laboratory. We guard against laser isotope effects by removing product gases from the laser beam path as rapidly as possible. During all of our measurements, the reaction chamber is exposed to a liquid nitrogen cold trap (CT 1, Fig. 2). Product SF_6, a condensable gas at liquid nitrogen temperatures, freezes out of the laser beam path and into the cold trap as soon as it is formed, thus minimizing interaction between SF_6 and laser light.

6.3. Control of F_2 Pressure on $\delta^{34}S_{V\text{-}CDT}$ and $\Delta^{33}S$

Rumble et al. (1993) showed $\delta^{34}S_{V\text{-}CDT}$ and $\Delta^{33}S$ to be independent of F_2 pressure from 20 to 130 torr for whole-grain analyses with a CO_2 laser. Similarly, $\delta^{34}S_{V\text{-}CDT}$ and $\Delta^{33}S_{V\text{-}CDT}$ values are independent of F_2 pressure from 15 to 65 torr for in

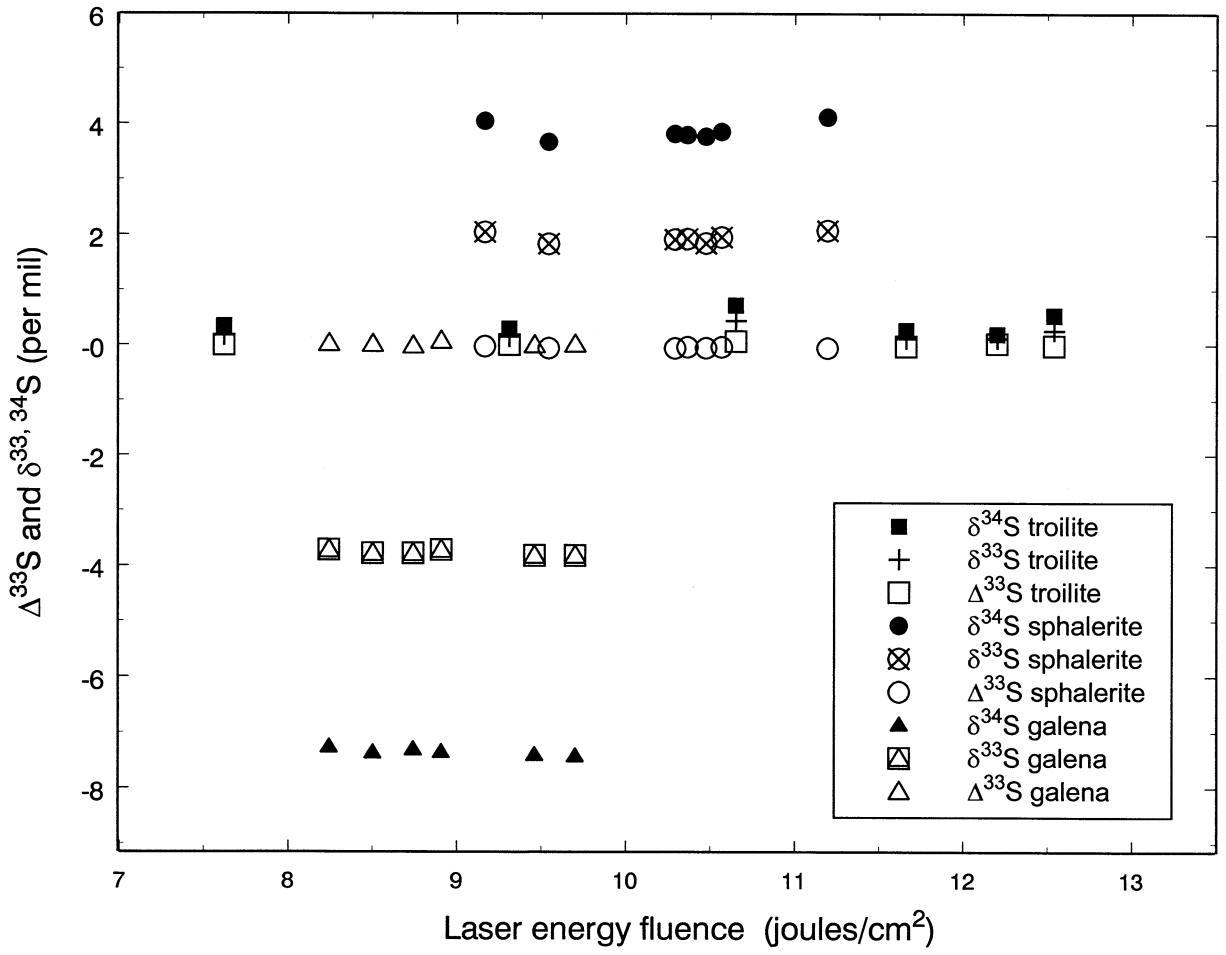

Fig. 10. Delta values plotted vs. KrF laser energy fluence ($\lambda = 248$ nm). Isotope values are independent of energy fluence. $\Delta^{33}S_{V\text{-}CDT}$ is zero within $\pm 0.07‰$.

situ analysis with a KrF excimer laser (Fig. 11). Use of low F_2 pressure is desirable to minimize spontaneous fluorination reactions, to speed the condensation of SF_6 into the liquid nitrogen cold trap, and to simplify fluorine passivation after lasing has ceased. But it is necessary to maintain a stoichiometric excess of F_2 in relation to the amount of SF_6 that is formed to ensure that fluorination is driven toward completion. A pressure of 20 torr F_2 is used for in situ analysis.

Beaudoin and Taylor (1994) observed that $\delta^{34}S$ values were a function of F_2 pressure at $P_{F_2} < 150$ torr and were independent of F_2 pressure at $P_{F_2} > 150$ torr with their MILES laser probe. We used much lower F_2 pressures and obtained the same values for the reference materials as Beaudoin and Taylor (1994); we did not observe changes in $\delta^{34}S_{V\text{-}CDT}$ and $\delta^{33}S_{V\text{-}CDT}$ values with changing F_2 pressure. Our method of analysis differed from that of Beaudoin and Taylor (1994) in that we trapped SF_6 in a liquid nitrogen cold trap (CT 1, Fig. 2) as soon as it formed, removing it from interaction with laser light immediately upon formation. Beaudoin and Taylor (1994) did not transfer SF_6 into a cryogenic trap until the termination of laser fluorination; thus, in their experiments, SF_6 was permitted to interact with the laser beam throughout the duration of lasing.

7. SULFUR ISOTOPE ANOMALIES IN ARCHEAN AND PALEOPROTEROZOIC SULFIDE MINERALS

The report by Farquhar et al. (2000) of anomalous mass-independent sulfur isotope fractionations in Archean and Paleoproterozoic sulfide and sulfate minerals may prove to equal in its impact on geochemistry the seminal finding by Clayton et al. (1973) of mass-independent oxygen isotope fractionation in meteorites. The restriction of the anomalies to rocks older than ~2.3 Ga, their absence in post-2.0-Ga sediments, and the coincidence of this transition with the time proposed for the oxygenation of Earth's atmosphere suggest the possible existence of a previously unrecognized quantitative geologic record of atmospheric evolution (Farquhar et al., 2000; Kasting, 2001). The discovery has been challenged by Ohmoto et al. (2001), who questioned the accuracy of the isotopic analyses of sulfur-bearing minerals. The existence of such anomalies, however, has been verified by direct ion probe measurements of both sulfide and sulfate minerals in Archean samples (Mojzsis et al., 2001; Runnegar, 2001). We have analyzed aliquots of Farquhar et al's (2000) powdered Ag_2S samples with the new CO_2 laser microprobe. The results of replicate analyses of 12 Ag_2S samples previously analyzed by Farquhar et al. (2000) are

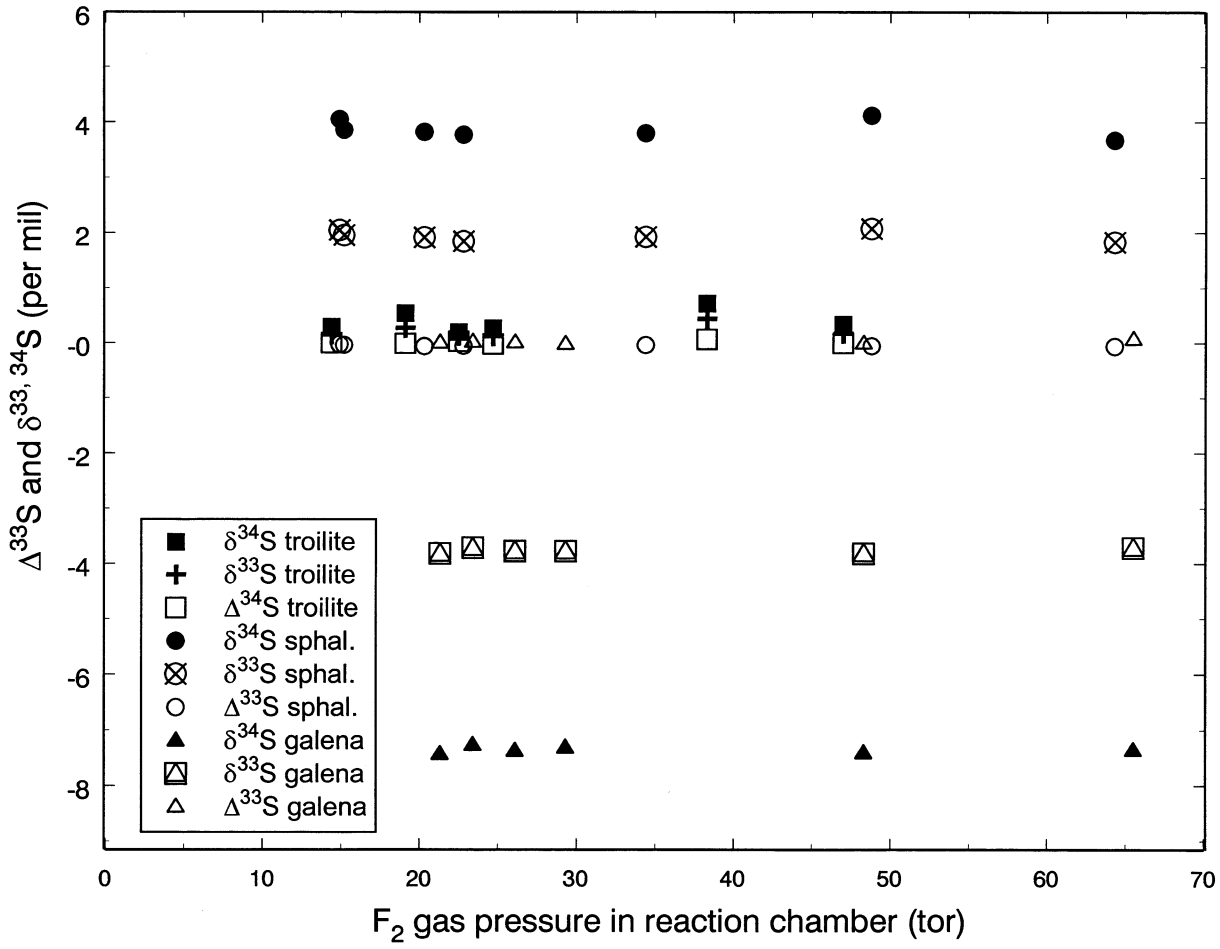

Fig. 11. Delta values plotted vs. F_2 gas pressure loaded into reaction chamber for KrF laser analysis. Isotope values are independent of F_2 pressure. $\Delta^{33}S_{V\text{-}CDT}$ is zero within $\pm 0.07‰$.

Table 4. Comparison of replicate analyses of Ag_2S samples between Geophysical Laboratory (GL) and University of California, San Diego (UCSD). GL samples measured with CO_2 laser; UCSD samples measured by bulk fluorination. Original samples obtained by courtesy of J. W. Schopf University of California, Los Angeles. Values reported to two decimals to facilitate comparison with published data.

	GL[a]			UCSD[b]		
Sample	$\delta^{33}S$ (‰)	$\delta^{34}S$ (‰)	$\Delta^{33}S$ (‰)	$\delta^{33}S$ (‰)	$\delta^{34}S$ (‰)	$\Delta^{33}S$ (‰)
pprg199-py	2.75	2.64	1.39	2.46	2.29	1.28
pprg199-sulfate	1.33	0.69	0.97	1.44	0.74	1.06
pprg212-pyrite	0.72	0.96	0.23	0.73	1.04	0.19
pprg486-sulfate	0.05	1.43	–0.69	0.00	1.33	–0.70
pprg1274-pyrite	10.53	20.58	–0.07	10.64	20.76	–0.06
pprg1410-pyrite	3.28	6.11	0.13	3.20	6.01	0.09
pprg1932-sulfate	2.03	0.30	1.88	2.04	0.30	1.89
pprg1932-py	1.28	–0.68	1.63	1.26	–0.68	1.62
pprg2447-pyrite	3.13	5.88	0.10	3.30	6.33	0.02
SAF-9-6-barite	1.90	4.46	–0.40	1.81	4.33	–0.43
pprg1411	1.53	2.99	–0.01	0.99	2.10	–0.10
pprg1419-pyrite	1.66	1.72	0.77	2.25	2.98	0.70

[a] This study.
[b] Farquhar et al (2000a).

Table 5. Archean sulfide minerals analyzed with KrF excimer laser.

Locality	Sample	$\delta^{33}S_{V\text{-}CDT}$	$\delta^{34}S_{V\text{-}CDT}$	$\Delta^{33}S$
Isua, Greenland[a]	Pyrite	–0.5	0.8	–0.87
Quartz-biotite gneiss 3.8 Ga	Pyrite	–0.3	1.1	–0.84
	Pyrite-quartz	0.2	2.1	–0.86
	Pyrite-biotite-Quartz	2.1	5.8	–0.85
Isua, Greenland[a]	Galena	–1.7	–3.1	–0.15
South Africa[b]	Pyrite	–0.8	–1.7	0.12
Lokamanno Fm.	Pyrite	–5.9	–8.5	–1.54
Schmidtsdrif Group 2.642 Ga	Pyrite	7.8	10.9	2.12
	Pyrite	7.9	9.6	2.95
	Pyrite	8.0	9.6	2.99
North Pole, Australia[c]	Pyrite	0.1	0.8	–0.28
Pilbara craton 3.5 Ga	Pyrite	0.6	1.8	–0.29
	Pyrite	0.2	1.1	–0.37
	Pyrite	0.1	0.8	–0.35
	Pyrite	0.2	1.0	–0.32
	Pyrite	0.4	1.4	–0.30

[a] Samples from M. Rosing; analyst G. Hu.
[b] Samples from H.D. Holland and A. Bekker; analysts A. Bekker and D. Rumble
[c] Samples from S. Maruyama and Y. Ueno; analysts Y. Ueno and G. Hu.

shown in Table 4. Except for samples pprg1411 and pprg1419-py, the $\delta^{34}S$ values of samples agree within ±0.2‰, and $\Delta^{33}S$ values agree within ±0.07‰. Although the differences between the $\delta^{34}S$ values for pprg1411 and pprg1419-py measured in the two laboratories are 0.9 and 1.2‰, respectively, the $\Delta^{33}S$ values agree within ±0.07‰. Note that our CO_2 laser analyses of IAEA reference materials and their agreement with other laboratories reported in Tables 1 and 2 provides an interlaboratory confirmation of Farquhar et al's (2000) data given in Table 4. Further confirmation of sulfur isotope anomalies is demonstrated below by direct, in situ spot analyses of pyrite with the new KrF excimer laser microprobe. There is no reason to doubt the existence of Archean and Paleoproterozoic mass-independent sulfur isotope fractionations on the grounds of incorrect analyses.

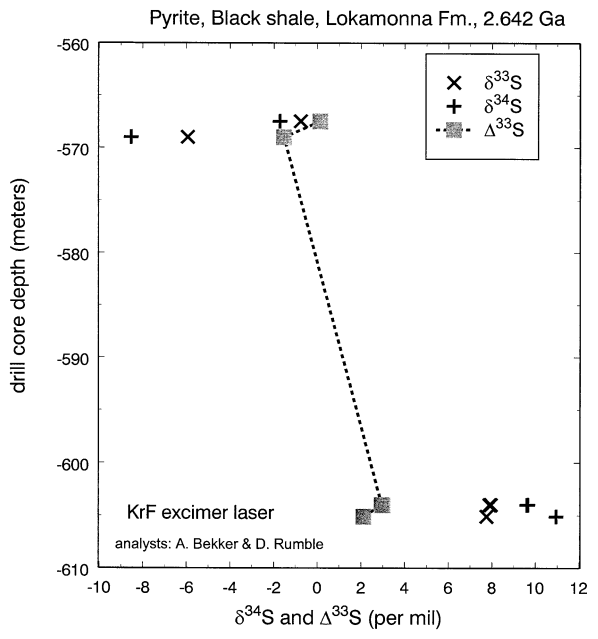

Fig. 12. Isotope profile of drill core through black shale, Lokamonna Formation, South Africa (Table 5) (2.642 Ga). Distances separating closely spaced samples have been exaggerated for clarity. Note shifts in isotope values over centimeter distances at both top and bottom of core. (Samples from H. D. Holland and A. Bekker; analyses by A. Bekker and D. Rumble).

We present below examples of the use of a UV laser fluorination analytical system to measure the stratigraphic distribution of sulfur isotope anomalies in drill core samples. The use of the system to locate and analyze specific mineral grains that preserve sulfur isotope anomalies is also illustrated.

The location and analysis of individual minerals hosting sulfur isotope mass-independent fractionations with the KrF excimer laser is illustrated by data on pyrite and galena from 3.8 Ga metasediments from Isua, Greenland (samples by courtesy of M. Rosing). A pyrite grain in quartz-biotite gneiss has $\delta^{33}S$ values of −0.5 to −0.3‰ and $\delta^{34}S$ values of of 0.8 to 1.1‰, with $\Delta^{33}S = -0.87$ to −0.84‰ (Fig. 9, Table 5). Galena from a mineralized zone in amphibolite gives $\delta^{33}S$ of –1.7‰ and $\delta^{34}S$ of –3.1‰, with $\Delta^{33}S = -0.15$‰ (Table 5). Aliquots of the galena contain examples of the most primitive terrestrial leads known (Appel et al., 1978; Richards and Appel, 1987).

The KrF excimer laser was used to analyze discoidal chips from an unweathered drill core of black shale from the Lokamonna Formation, Schmidtsdrif Group, South Africa, with an age of ~2.642 ± 3 Ga (core samples collected by H. D. Holland, analyses by A. Bekker and D. Rumble) (Table 5). Over a 37-m depth interval, $\delta^{34}S$ varies from −8.5 to +10.9‰ and $\Delta^{33}S$ ranges from –1.5 to +3.0‰ (Fig. 12, Table 5). Note that closely spaced black shale beds vary in $\Delta^{33}S$ from +0.1 to –1.5‰ at the top of the core and from +2.1 to +3.0 at the bottom (Fig. 12). The entire range of published variations in $\Delta^{33}S$ (Farquhar et al., 2000) is thus seen to reside in a 37-m length of drill core. These results with a KrF excimer laser

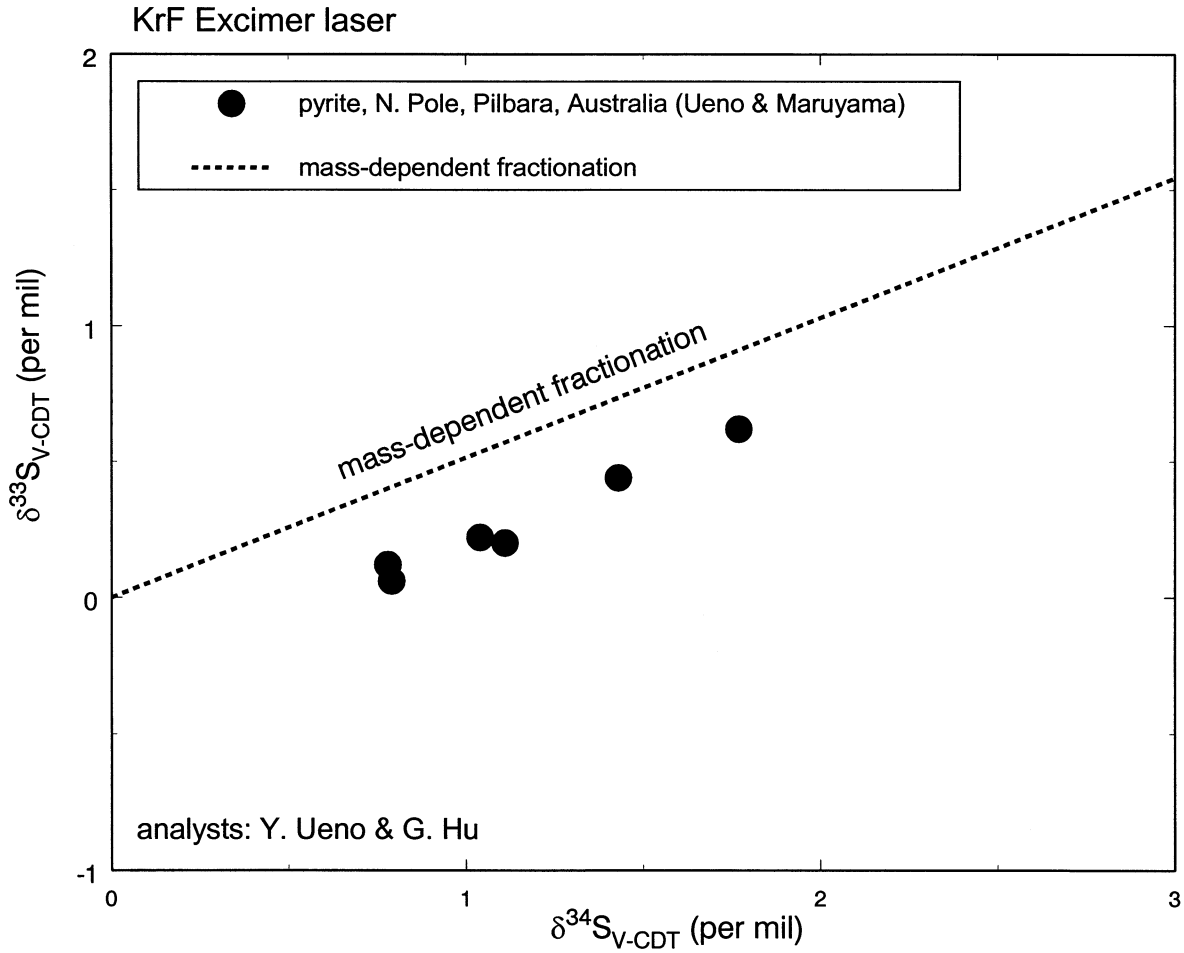

Fig. 13. Sulfur isotope values of pyrite grains from same bed of 3.5 Ga chert, North Pole, Pilbara Craton, Australia (Table 5). Analyses plot on line parallel to mass-dependent trend of interlaboratory reference materials but are offset from it. (Samples from S. Maruyama and Y. Ueno; analysts Y. Ueno and G. Hu).

suggest that full resolution of stratigraphic variations in sulfur isotope anomalies may require analyses spaced as closely as a few centimeters apart.

In another example, we explored the capabilities of the KrF excimer laser for spatially resolved sulfur isotope analyses of individual pyrite grains (Fig. 13, Table 5). Samples from the 3.5 Ga North Pole district, Pilbara Craton, Australia, are either hand picked, individual pyrite grains or pyrite analyzed in situ in bedded chert, all from the same stratigraphic horizon. The $\delta^{34}S_{V\text{-}CDT}$ values of pyrite grains are variable, ranging from +0.8 to +1.8‰ (Table 3). All pyrites, however, have $\Delta^{33}S = -0.32 \pm 0.04$‰ (Fig. 13).

A striking feature of the sulfur isotopic compositions of pyrite samples from North Pole is the homogeneity of $\Delta^{33}S$ values over a centimeter length scale but a contrasting millimeter-scale heterogeneity of $\delta^{34}S$ between sulfide grains (Fig. 13). These features strongly resemble the secondary equilibration oxygen isotope arrays discovered by Clayton and Mayeda (1996) for planetary bodies (i.e., Earth-Moon, SNC, and HED correlated arrays plotted on $\delta^{17}O$ vs. $\delta^{18}O$ diagrams). Establishment of protolith mass-independent isotopic compositions, whether in a sedimentary bed or in a planetary body, was followed by local mass-dependent fractionation processes for both sulfur and oxygen isotopes.

We draw attention to an additional parallel between Archean $\delta^{33}S$ vs. $\delta^{34}S$ and meteorite $\delta^{17}O$ vs. $\delta^{18}O$ systematics. Primordial differences in $\Delta^{17}O$ are known to survive in chondritic meteorites despite parent body metamorphism (Clayton et al., 1991). Measurements of the Lokamonna black shale drill core, pyrites from North Pole chert, and pyrite and galena from Isua metasediments suggest that protolith differences in $\Delta^{33}S$ may survive despite postsedimentation alteration and metamorphism.

The variations in $\delta^{34}S$ values between individual pyrite grains over short distances in Archean rocks measured with a KrF excimer laser are not unprecedented. Ohmoto et al. (1993) reported a range in $\delta^{34}S$ of –3.0 to +8.6‰ in pyrite grains from 3.4 Ga black shale and black chert of the Onverwacht group, Barberton Greenstone Belt, South Africa, measured with Nd:YAG (yttrium aluminum garnet) laser oxidation (cf. Kakegawa et al., 1999; Kakegawa and Ohmoto, 1999). These variations were interpreted as evidence of sulfur isotope fractionation by microbes living at the time of sediment deposition (Ohmoto et al., 1993). Our discovery of variable $\delta^{34}S$ but constant $\Delta^{33}S$ in

pyrites from a single sedimentary bed at North Pole, Pilbara, supports the interpretation of biogenic sulfur isotope fractionation. Photochemical fractionation would lead to correlated $\delta^{34}S$ and $\Delta^{33}S$ mass-independent variations according to the experiments of Farquhar et al. (2001a). Biogenic fractionation, however, should be mass dependent (Farquhar et al., 2001b), as shown in Figure 13.

Our discovery in drill core samples of millimeter- to centimeter- to meter-scale variations in $\delta^{34}S$ values accompanied by large shifts in $\Delta^{33}S$ (Fig. 12) suggests that caution should be exercised in interpreting Archean sulfur isotope systematics on the basis of analyses of $\delta^{34}S$ alone. Prudence requires rigorous testing of a number of working hypotheses, including biogenic fractionation and non-mass-dependent fractionation by analyzing at least three of the four stable sulfur isotopes. Inorganic isotope fractionation mechanisms should be evaluated as well on the basis of geological, mineralogical, chemical, and isotopic data (Ohmoto and Goldhaber, 1997; Canfield, 2001). The door should be left open for consideration of new working hypotheses to be inspired by as yet unanticipated discoveries made by exploiting the capabilities of multisulfur isotope analysis.

8. SUMMARY

A new KrF excimer and CO_2 laser microprobe was constructed for the analysis of multisulfur isotopes. The analysis of powdered sulfides can be achieved with an accuracy and precision of 0.2‰ for $\delta^{34}S_{V\text{-}CDT}$ and $\delta^{33}S_{V\text{-}CDT}$ on the basis of IAEA and NIST interlaboratory isotope reference materials, as demonstrated by Rumble et al. (1993) and Beaudoin and Taylor (1994). In situ spot analysis with a KrF excimer laser yields values for $\delta^{34}S_{V\text{-}CDT}$ and $\delta^{33}S_{V\text{-}CDT}$ with an accuracy and precision of 0.2‰ for pyrite, sphalerite, galena, troilite, and chalcopyrite. Values of $\Delta^{33}S$ are measured to ± 0.07‰ (cf. Clayton and Mayeda, 1996, for $\Delta^{17}O$). Both $\delta^{34}S_{V\text{-}CDT}$ and $\delta^{33}S_{V\text{-}CDT}$ are independent of F_2 pressure and laser energy fluence. No mineral-specific fractionation correction for measured sulfur isotope compositions is needed.

Direct measurements of sulfur isotopic compositions of Archean pyrites made with a KrF excimer laser microprobe confirm the existence of nonzero $\Delta^{33}S$ sulfur isotope anomalies as large as +3.0‰ and as small as –1.5‰. Correlated arrays of $\delta^{33}S$ vs. $\delta^{34}S$ with slope +0.5 and $\Delta^{33}S \neq 0$ have been found that resemble the postaccretion equilibration arrays in $\delta^{17}O$ vs. $\delta^{18}O$ discovered in meteorites by Clayton and Mayeda (1996). Preliminary results on the Archean stratigraphic distribution of sulfur isotope anomalies show that the entire known range of variation in $\Delta^{33}S$ may occur in a short length of drill core.

Acknowledgments—The authors thank A. Bekker, G. D. Cody, P. G. Conrad, J. Farquhar, M. L. Fogel, H. D. Holland, W. T. Huntress, J. Kasting, S. Maruyama, K. Nealson, H. Ohmoto, S. Ono, M. Rosing, J. W. Schopf, J. Scott, B. E. Taylor, Y. Ueno, and B. Wing for providing Archean samples and for helpful discussions. We thank G. L. Kim for graciously sharing use of the excimer laser. This study and the cost of building the UV laser microprobe were supported by contract 1213932 from the Jet Propulsion Laboratory's Grand Challenge Program to K. Nealson and P. G. Conrad (JPL-USC) and to M. L. Fogel, W. T. Huntress, and D. Rumble (Geophysical Laboratory). Manuscript reviews by D. E. Crowe, A. E. Fallick, and J. Horita were helpful.

Associate editor: J. Horita

DEDICATION

The authors honor the many inspiring and exciting research discoveries of R. N. Clayton and wish to dedicate this work to him. Clayton's pioneering research on ^{16}O-^{17}O-^{18}O systematics in meteorites is proving to be an instructive road map for exploring ^{32}S-^{33}S-^{34}S-^{36}S systematics in terrestrial sulfide minerals, as shown by the examples presented in this paper.

REFERENCES

Appel P. W. U., Moorbath S., and Taylor P. N. (1978) Least radiogenic terrestrial lead from Isua, West Greenland. *Nature* **272,** 524–526.

Asprey L. B. (1976) The preparation of very pure fluorine gas. *J. Fluor. Chem.* **7,** 359–361.

Bains-Sahota S. K. and Thiemens M. H. (1988) Fluorination of SF_4, SF_5Cl, and S_2F_{10} to SF_6 for mass spectrometric isotope ratio analysis. *Anal. Chem.* **60,** 1084–1086.

Beaudoin G. and Taylor B. E. (1994) High precision and spatial resolution sulfur isotope analysis using MILES laser microprobe. *Geochim. Cosmochim. Acta* **58,** 5055–5063.

Canfield D. E. (2001) Biogeochemistry of sulfur isotopes. *Rev. Mineral. Geochem.* **43,** 607–636.

Chaussidon M., Albarede F., and Sheppard S. M. F. (1989) Sulfur isotope variations in the mantle from ion microprobe analyses of micro-sulfide inclusions. *Earth Planet. Sci. Lett.* **92,** 144–156.

Clayton R. N., Grossman L., and Mayeda T. K. (1973) A component of primitive nuclear composition in carbonaceous meteorites. *Science* **182,** 485–488.

Clayton R. N., Mayeda T. K., Goswani J. N., and Olsen E. J. (1991) Oxygen isotope studies of ordinary chondrites. *Geochim. Cosmochim. Acta* **55,** 2317–2337.

Clayton R. N. and Mayeda T. K. (1996) Oxygen isotope studies of achondrites. *Geochim. Cosmochim. Acta* **60,** 1999–2017.

Coplen T. B. and Krouse H. R. (1998) Sulphur isotope data consistency improved. *Nature* **392,** 32.

Crowe D. E., Valley J. W., and Baker K. L. (1990) Micro-analysis of sulfur-isotope ratios and zonation by laser microprobe. *Geochim. Cosmochim. Acta* **54,** 2075–2092.

Ding T., Valkiers S., Kipphardt H., De Bievre P., Taylor P. D. P., Gonfiantini R., and Krouse R. (2001) Calibrated sulfur isotope abundance ratios of three IAEA sulfur isotope reference materials and V-CDT with a reassessment of the atomic weight of sulfur. *Geochim. Cosmochim. Acta* **65,** 2433–2437.

Eldridge C. S., Compston W., Williams I. S., and Walshe J. L. (1989) Sulfur isotope analyses on the SHRIMP ion probe. *U.S. Geol. Surv. Bull.* **1890,** 163–174.

Farquhar J. and Rumble D. (1998) Comparison of oxygen isotope data obtained by laser fluorination of olivine with a KrF excimer laser and CO_2 laser. *Geochim. Cosmochim. Acta* **62,** 3141–3149.

Farquhar J., Bao H., and Thiemens M. H. (2000) Atmospheric influence of Earth's earliest sulfur cycle. *Science* **289,** 756–758.

Farquhar J., Savarino J., Airieau S., and Thiemens M. H. (2001a) Observation of wavelength-sensitive mass-independent sulfur isotope effects during SO_2 photolysis: Implications for the early atmosphere. *J. Geophys. Res.* **106,** 32829–32839.

Farquhar J., Airieau S., Thiemens M. H., Canfield D., Habicht K. (2001b) Considerations for evaluation of isotopic evidence for biological activity. National Astrobiology Institute, Abstracts of First Annual Meeting.

Farquhar J., Bao H., Thiemens M. H., Hu G., Rumble D. (2001c) Technical comment: Questions regarding Precambrian sulfur isotope fractionation: Response. Science **292,** 1959a.

Fiebig J., Wiechert U., Rumble D., and Hoefs J. (1999) High-precision in situ oxygen isotope analysis of quartz using an ArF laser. *Geochim. Cosmochim. Acta* **63,** 687–702.

Gao X. and Thiemens M. H. (1991) Systematic study of sulfur isotopic composition in iron meteorites and the occurrence of excess ^{33}S and ^{36}S. *Geochim. Cosmochim. Acta* **55,** 2671–2679.

Greenwood J. P., Mojzsis S. J., and Coath C. D. (2000) Sulfur isotopic compositions of individual sulfides in Martian meteorites ALH84001

and Nakhla: Implications for crust-regolith exchange on Mars. *Earth Planet. Sci. Lett.* **184,** 23–35.

Hayes J. M., Lambert I. B., and Strauss H. (1992) The sulfur-isotope record. In *The Proterozoic Biosphere* (eds. J. W. Schopf and C. Klein) pp. 129–156. Cambridge University Press, New York.

Hulston J. R. and Thode H. G. (1965) Variations in the S^{33}, S^{34}, and S^{36} contents of meteorites and their relation to chemical and nuclear effects. *J. Geophys. Res.* **70,** 3475–3484.

Ilchik R. P. and Rumble D. (2000) Sulfur, carbon, and oxygen isotope geochemistry of pyrite and calcite from veins and sediments sampled by borehole CCM-2, Creede Caldera, Colorado. In *Ancient Lake Creede; Its Volcano-Tectonic Setting, History of Sedimentation, and Relation to Mineralization in the Creede Mining District* (ed. P. M. Bethke) vol. 346, pp. 287–300. Geological Society of America, Washington, DC.

Kakegawa T. and Ohmoto H. (1999) Sulfur isotope evidence for the origin of 3.4 to 3.1 Ga pyrite at the Princeton gold mine, Barberton Greenstone Belt, South Africa. Hammersly District, Western Australia.. *Precam. Res.* **96,** 209–224.

Kakegawa T., Kawai H., and Ohmoto H. (1999) Origin of pyrites in the 2.5 Ga Mt. McRae shale, Hammersly district, Western Australia. *Geochim. Cosmochim. Acta* **62,** 3205–3220.

Kasting J. F. (2001) The rise of atmospheric oxygen. *Science* **293,** 819–820.

Kelley S. P. and Fallick A. E. (1990) High precision spatially resolved analysis of $\delta^{34}S$ in sulfides using a laser extraction technique. *Geochim. Cosmochim. Acta* **54,** 883–888.

Letokhov V. S. (1979) Laser isotope separation. *Nature* **277,** 605–610.

Lyman J. L., Jensen R. J., Rink J., Robinson C. P., and Rockwood S. D. (1975) Isotopic enrichment of SF_6 in ^{34}S by multiple absorption of CO_2 laser radiation. *Appl. Phys. Lett.* **27,** 87–89.

McKibben M. A. and Riciputi L. R. (1998) Sulfur isotopes by ion probe. *Rev. Econ. Geol.* **7,** 121–139.

Mojzsis S. J., Coath C. D., Greenwood J. P., McKeegan K. D., Harrison T. M., Runnegar B. (2001) Non-mass-dependent sulfur isotopes documented from in situ measurements of Precambrian sedimentary sulfides by multi-collector ion microprobe. Goldschmidt Conference, A3185.

Monster J., Appel P. W. U., Thode H. G., Schidlowski M., Carmichael C. M., and Bridgwater D. (1979) Sulfur isotope studies in early Archean sediments from Isua, West Greenland: Implications for the antiquity of bacterial sulfate reduction. *Geochim. Cosmochim. Acta* **43,** 405–413.

Ohmoto H. and Goldhaber M. B. (1997) Sulfur and carbon isotopes. In *Geochemistry of Hydrothermal Ore Deposits*. (ed. H. L. Barnes). John Wiley, New York, pp. 517–611.

Ohmoto H., Kakegawa T., and Lowe D. R. (1993) 3.4-billion-year-old biogenic pyrites from Barberton, South Africa: Sulfur isotope evidence. *Science* **262,** 555–557.

Ohmoto H., Yamaguchi K., Ono S. (2001) Technical comment: Questions regarding Precambrian sulfur isotope fractionation. Science **292,** 1959a.

Oi T., Taguma N., and Kakihana H. (1985) Calculation of thermodynamic sulfur isotope effect. *J. Nucl. Sci. Tech.* **22,** 818–832.

Rees C. E. (1978) Sulphur isotope measurements using SO_2 and SF_6. *Geochim. Cosmochim. Acta* **42,** 383–389.

Richards J. R. and Appel P. W. U. (1987) Age of the "least radiogenic" galenas at Isua, West Greenland. *Chem. Geol.* **66,** 181–191.

Romero A. B., Thiemens M. (2000) Mass-independent sulfur isotopic compositions in sulfate aerosols: implications for atmospheric chemistry and sulfate deposition. EOS (2000) Fall Meeting, F38.

Rumble D., Hoering T. C., and Palin J. M. (1993) Preparation of SF_6 for sulfur isotope analysis by laser heating sulfide minerals in the presence of F_2 gas. *Geochim. Cosmochim. Acta* **57,** 4499–4512.

Rumble D., Farquhar J., Young E. D., and Christensen C. P. (1997) In situ oxygen isotope analysis with an excimer laser using F_2 and BrF_5 reagents and O_2 gas as analyte. *Geochim. Cosmochim. Acta* **61,** 4229–4234.

Runnegar B. (2001) Archean sulfates from Western Australia: Implications for Earth's early atmosphere and ocean. Goldschmidt Conference 11, A3859.

Sato K. (1984) Reflectivity spectra and optical constants of pyrites (FeS_2, CoS_2, and NiS_2) between 0.2 and 4.4 eV. *J. Phys. Soc. Jap.* **53,** 1617–1620.

Shanks W. C., Crowe D. E., and Johnson C. (1998) Sulfur isotope analyses using the laser microprobe. *Rev. Econ. Geol.* **7,** 141–153.

Sharp Z. D. (1990) A laser-based microanalytical method for in situ determination of oxygen isotope ratios of silicates and oxides. *Geochim. Cosmochim. Acta* **54,** 1353–1358.

Shen Y., Buick R., and Canfield D. E. (2001) Isotopic evidence for microbial sulphate reduction in the early Archean era. *Nature* **410,** 77–81.

Taylor B. E. (in press) Laser-assisted micro-analysis of the sulfur isotope reference materials using the SF_6 method: Calibration of the sulfur isotope reference scale and consistent discrepancies with SO_2-based measurements. In International Atomic Energy Agency, Vienna, IAEA-TECDOC.

Thiemens M. H. (1999) Mass-independent isotope effects in planetary atmospheres and the early solar system. *Science* **283,** 341–345.

Thiemens M. H. (2001) Mass independent isotopic compositions of aerosol sulfate and nitrates. *Eos: Trans. Am. Geophys. Union* **82,** F70.

Thode H. G. and Goodwin A. M. (1983) Further sulfur and oxygen isotope studies of late Archean iron-formations of the Canadian Shield and the rise of sulfate reducing bacteria. *Precam. Res.* **20,** 337–356.

Wiechert U. and Hoefs J. (1995) An excimer laser-based micro analytical preparation technique for in-situ oxygen isotope analysis of silicate and oxide minerals. *Geochim. Cosmochim. Acta* **59,** 4093–4101.

Young E. D., Coutts D. W., and Kapitan D. (1998) UV laser ablation and irm-GCMS microanalysis of $^{18}O/^{16}O$ and $^{17}O/^{16}O$ with application to a calcium-aluminum-rich inclusion from the Allende meteorite. *Geochim. Cosmochim. Acta* **62,** 3161–3168.

Zmolek P., Xu X. P., Jackson T., Thiemens M. H., and Trogler W. C. (1999) Large mass independent sulfur isotope fractionations during photopolymerization of CS_2-^{12}C and CS_2-^{13}C. *J. Phys. Chem.* **103,** 2477–2480.